

Validation of 0.25° x 0.25° Indian Ocean HYCOM

Sudheer Joseph and M. Ravichandran

*Indian National Centre for Ocean Information Services,
Hyderabad*

Contents

1	Introduction	1
2	The Model configuration	2
3	Climatological Simulation	2
3.1	Flux Correction	2
4	Inter-annual NOGAPS atmospheric forcing parameters	4
4.1	Statistical Parameters	4
5	Inter Annual Simulation and Validation	6
5.1	Sea Level Anomalies (SLA)	6
5.2	Currents	12
5.3	Sea Surface Temperature (SST)	21
5.4	Vertical Profiles of Temperature	28
6	Conclusions	37
7	Acknowledgements	39

List of Figures

1	Basin Average Kinetic Energy stabilization during 10 year climatological simulation	3
2	Annual mean error of HYCOM climatological SST from 4 th year with respect to Path finder SST before correction (left) and after correction (right)	3
3	NOGAPS Zonal (Top) Meridional(Bottom) wind comparison with winds from RAMA buoy in Bay of Bengal	5
4	RMS difference between HYCOM SLA and altimeter SLA for the period 2003–2010.	7
5	Correlation of HYCOM SLA with altimeter SLA for the period 2003–2010	9
6	Selected Sample locations were daily SLA time-series where chosen for validation	10
7	Comparison of HYCOM SLA with altimeter SLA time-series at Equatorial Indian Ocean and Arabian Sea locations	10
8	Comparison of HYCOM SLA with altimeter SLA time-series at Equatorial Indian Ocean and Bay of Bengal locations	11
9	Evolution of OSCAR (top) and model (bottom) currents during January to April	13
10	Evolution of OSCAR (top) and HYCOM (bottom) currents during May to August	14
11	Evolution of OSCAR (top) and HYCOM (bottom) currents during September to December	16
12	Location of RAMA buoys selected for comparison of Currents and calculating statistics	17
13	RAMA-BUOYS selected for comparison of Currents and calculating statistics in equatorial Indian Ocean locations	19
14	RAMA-BUOYS selected for comparison of Currents and calculating statistics in equatorial Indian Ocean locations	20
15	HYCOM SST RMS difference with TMI SST	22
16	HYCOM SST Correlation with TMI SST	23
17	Location map for RAMA buoys used for SST validation	25
18	Comparison of SST from selected RAMA-BUOYS and HYCOM SST interpolated to the location of each. Corresponding statistics are presented in Table - 4	27
19	Time depth section of RAMA mooring at 90° E 15° N compared against HYCOM temperature sampled at same location.	28
20	Time depth section of RAMA mooring at 90° E 12° N compared against HYCOM temperature sampled at same location	29
21	Time depth section of RAMA mooring at 80.5° E 0° N compared against HYCOM temperature sampled at same location	30
22	Spatial correlation scale of temperature at a depth of 200 m at 80.5° E 0° N	31

23	Time depth section of Argo float 2900556 compared against HYCOM temperature sampled at same locations and time	32
24	Time depth section of Argo float 2900552 compared against HYCOM temperature sampled at same location	33
25	Time depth section of Argo float 2900264 compared against HYCOM temperature sampled at same location	34
26	Time depth section of Argo float 2900755 compared against HYCOM temperature sampled at same location	35
27	Time depth section of Argo float 1900311 compared against HYCOM temperature sampled at same location	36
28	Quality flags of RAMA Buoy currents used for comparison with HYCOM current time series(R-01 to R-14 ,Figure-12)	43

List of Tables

1	Comparison of SLA Statistics from HYCOM and altimeter at locations marked in Figure - 6	11
2	Statistics of Rama buoy Zonal current velocities and same simulated by HYCOM extracted at same time ans space.	17
3	Statistics of Rama buoy meridional current velocities and same simulated by HYCOM extracted at same time ans space.	18
4	Statistics of Rama buoy SST and same simulated by HYCOM extracted at same time ans space.	26

Summary

First time in India, Hybrid Coordinate Model (HYCOM) is implemented on IBM Power 6 machine at INCOIS and configured for Indian Ocean basin with $0.25^\circ \times 0.25^\circ$ spatial resolution. Three hourly Navy Operational Global Atmospheric Prediction System (NOGAPS) based buoyancy and momentum fluxes with 0.5° spatial resolution were used for forcing the model. In this report we present the comparison the model simulated Sea level anomalies, Sea surface temperatures, currents and vertical profiles of temperature with those available from observational platforms and satellite data on a daily to monthly scale for the period 2003 to 2010. We present a critical analysis of model simulated variables and available observations and present the pluses and minuses of the model performance. We also make few suggestions for possible improvements in simulation, in view of the statistical evaluation of model variables.

1 Introduction

The HYbrid Coordinate Ocean Model (HYCOM) (*Halliwel, 1997; Bleck, 2002*) is a primitive equation general circulation model which is isopycnal in the open, stratified ocean, but uses the layered continuity equation to make a dynamically smooth transition to a terrain-following coordinate in shallow coastal regions, and to z-level coordinates in the mixed layer and/or unstratified seas. It maintains the significant advantages of an isopycnal model in stratified regions while allowing more vertical resolution near the surface and in shallow coastal areas, hence providing a better representation of the upper ocean physics. An ideal numerical ocean model should retain its water mass characteristics for centuries (typically done by isopycnic coordinates), have high vertical resolution in the surface mixed layer and maintain sufficient vertical resolution in unstratified or weakly stratified regions of the ocean (typical nature of depth coordinates), and have high vertical resolution in coastal regions (attained by terrain following coordinates). HYCOM is designed to provide a major advantage over the existing operational global ocean prediction systems, by integrating all the required characteristics of above oceanic realms and it overcomes design limitations of the present systems as well as limitations in vertical and horizontal resolution to a great extent.

Successful modeling efforts in Indian Ocean were limited due to the lack of adequate observations and complexities involved in this region. However *Haugen et al. (2002a,b)* modeled Indian Ocean using an isopycnic co-ordinate model called MYCOM (Miami Isopycnic Coordinate Model) and the results were promising. The generalized coordinate (hybrid) ocean model HYCOM retains many of the characteristics of its predecessor, the isopycnic coordinate model MICOM. The freedom to adjust the vertical spacing of the coordinate surfaces in HYCOM allows easier numerical implementation of several physical processes (mixed layer detrainment, convective adjustment, sea ice modeling,) without affecting the model of the basic and numerically efficient resolution of the vertical that is characteristic of isopycnic models throughout most of the ocean's volume.

With improvements implemented, HYCOM is expected to improve the performance and can be used for the operational needs in this region.

Internationally HYCOM is one of the most widely used model for operational oceanography, considering its potential to simulate the oceanic process close to the reality. Many leading navy's across the globe uses it for their operational requirements.

2 The Model configuration

HYCOM (*Bleck, 2002*) is configured for the Indian Ocean (20°E to 125°E and 35°S to 31°N) on a High Performance Computer (HPC) IBM Power 6 series system with AIX operating system. This model has a hybrid vertical coordinate, which is isopycnal in the open, interior and stratified ocean, while using a z-level coordinate in the mixed layer. It combines the advantages of isopycnic coordinates and z-level coordinates in a unique way to improve the simulations. The present configuration is with a 0.25° x 0.25° horizontal resolution, 28 hybrid layers in the vertical, and a nonlocal K-profile parameterization (KPP) is used for the boundary layer mixing scheme (*Large et al., 1994*). It has river run off included using the Naval Research Laboratory's monthly climatology (*Barron and Smedstad, 2002*). The model thermohaline fields are initialized with World Ocean Atlas climatology (*Antonov et al., 1998*) and the General Bathymetric Chart of the Oceans (GEBCO) data is used for bottom topography. The model is relaxed to climatology at its southern and eastern boundaries 50 E-folding days.

3 Climatological Simulation

The temperature and salinity climatology were interpolated to model grid from the world ocean Atlas version 98. The atmospheric forcing from NCEP were interpolated to 6 hourly temporal grid. Wind speed and wind stress curl were then augmented with 6 hourly anomalies for generating the high frequency variability with in the model. This approach prevents the model having sudden shock when the model is forced with realistic forcing during inter annual runs. The model has been spun up for 10 years as the region wide kinetic energy attained a stable state.

3.1 Flux Correction

In order to the correct for the bias due to atmospheric fluxes, an SST offset was computed after initial 4 years run with respect to pathfinder SST climatology and after applying the computed offset, the model was again spun up for 10 years. This method was applied to correct the model bias imposed by the atmospheric fluxes generated by numerical weather predication model (Figure - 2).

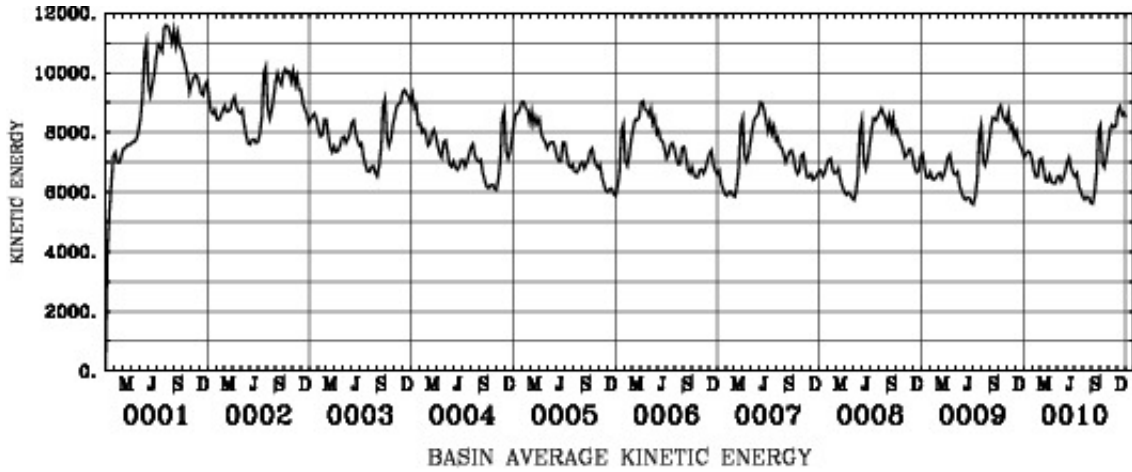


Figure 1: Basin Average Kinetic Energy stabilization during 10 year climatological simulation

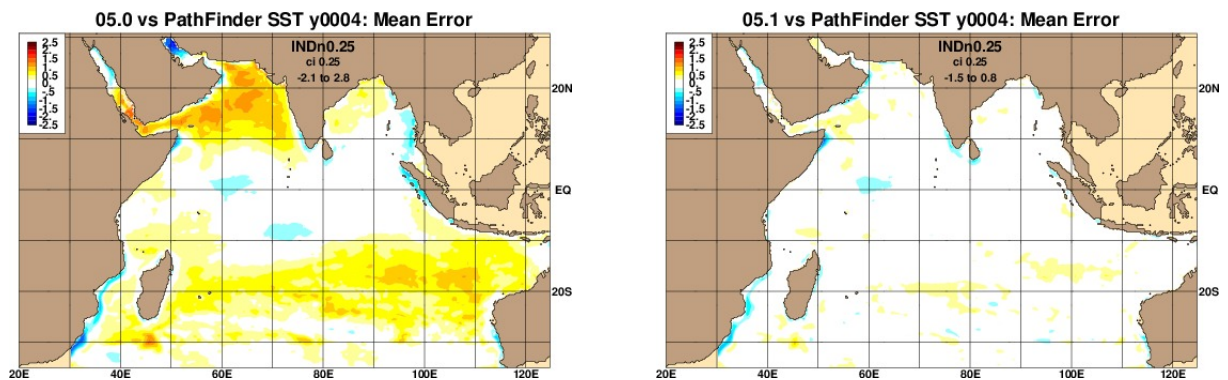


Figure 2: Annual mean error of HYCOM climatological SST from 4th year with respect to Path finder SST before correction (left) and after correction (right)

4 Inter-annual NOGAPS atmospheric forcing parameters

We used the following Fleet Numerical Meteorology and Oceanography Center (FNMOC) 3-hourly Navy Operational Global Atmospheric Prediction System (NOGAPS) buoyancy and momentum fields with $0.5^\circ \times 0.5^\circ$, spatial resolution for forcing HYCOM.

1. Air temperature at 2 m.
2. Surface specific humidity.
3. Net surface shortwave and long wave radiation.
4. total (large scale plus convective) precipitation.
5. Sea Surface Temperature.
6. zonal and meridional wind velocities at 10 m.
7. Mean sea level pressure and dew-point temperature at 2 m.

The first six parameters are input directly into the ocean model or used in calculating components of the heat and buoyancy fluxes while the last four are used to compute surface wind stress with temperature and humidity based stability dependence. As wind is one of the important parameter which need to be accurate enough to get realistic ocean simulation, we compared the zonal and meridional components of wind with those of Rama buoys and statistical evaluation showed that they are in good agreement (Figure- 3).

4.1 Statistical Parameters

In order to assess the realism of the simulation of different oceanic parameters presented in this report we used the statistical parameters viz. Mean Error (ME), Root Mean Square Difference (RMSD) Correlation (CORR) and non dimensional Skill Score (SS) following Kara et. al 2008.

$$ME = \bar{X} - \bar{Y} \quad (1)$$

$$RMSD = \left[\frac{1}{n} \sum_{i=1}^N (Y_i - X_i)^2 \right]^{\frac{1}{2}} \quad (2)$$

$$CORR = \sum_{i=1}^N (X_i - \bar{X})(Y_i - \bar{Y}) / \sigma_X \sigma_Y \quad (3)$$

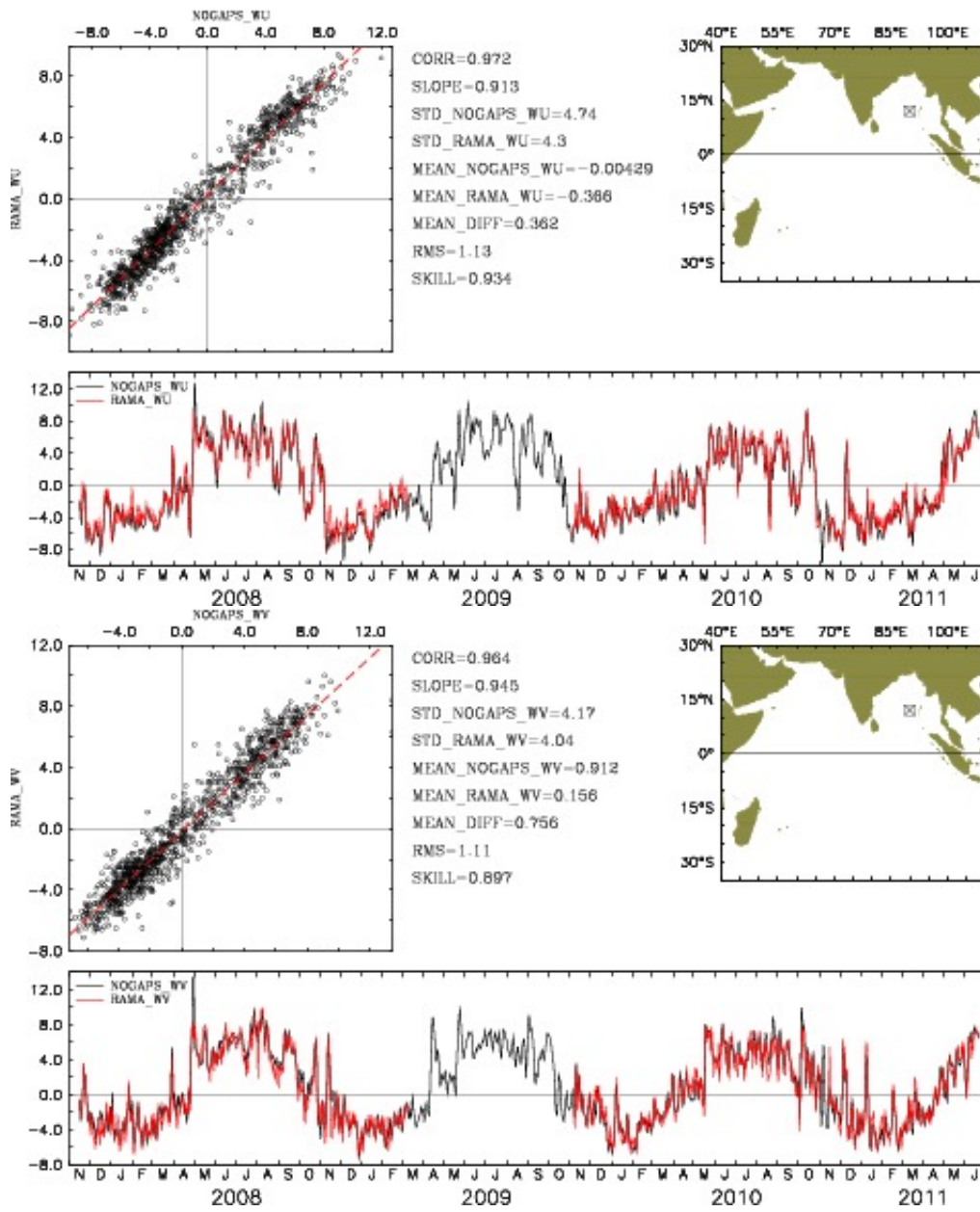


Figure 3: NOGAPS Zonal (Top) Meridional(Bottom) wind comparison with winds from RAMA buoy in Bay of Bengal

$$SS = R^2 - \underbrace{[R - (\sigma_Y/\sigma_X)]^2}_{\text{}} - \underbrace{[R - (\bar{Y} - \bar{X})/\sigma_X]^2}_{\text{}} \quad (4)$$

5 Inter Annual Simulation and Validation

After 10 years of climatological integration, HYCOM was inter-annually run using climatological restart file, for the period 2003 to 2011 using 3 hourly NOGAPS forcing parameters mentioned previously. Selected parameters from the inter-annual run for the period 2003 to 2010 is evaluated using available observations in the below sections.

5.1 Sea Level Anomalies (SLA)

Sea level is a parameter which reflects the realism in simulation of thermal, haline and wind driven circulation of an ocean general circulation model. If any of these fields become poor in their performance, the result will be a poor Sea level simulation by the model.

In order to assess the spatio temporal realism by which the model captures the sea level variability for the period 2003 to 2010, spatial statistics in terms of RMS difference and correlation were computed between HYCOM sea level anomalies and altimeter sea level anomalies from a delayed mode merged altimeter data product available from Archiving, Validation and Interpretation of Satellite Oceanographic Data (AVISO).

Figure-4, depicts the RMS difference between sea-level anomalies for each year for the period 2003–2010. The panels show the sea-level anomaly differences between the observed and model sea-level ranges from zero to 7 cm except for two highly dynamic western boundary regions in the model domain, the east African coast and western Bay of Bengal (east coast of India) where there are reported evidences of highly dynamic eddies. In these 2 dynamic regions, the RMS difference goes above 10 cm between model and altimeter sea level anomalies. For year 2003 the area covered with higher RMS difference (poor model simulation of sea level anomalies) is relatively larger in east African coastal region and BoB, which could be due the model inter annual start in same year from climatology. During 2004, the area of poor SLA simulation are seen more limited to the east African coast and also become less prominent in Bay of Bengal. The figure also demonstrate that there are certain amount of inter-annual variability in the RMS differences between the model and the observed sea-level anomalies by altimeter. This could be attributed to the inter-annual differences of the eddy activity in both locations. The correlation maps (Figure- 5)

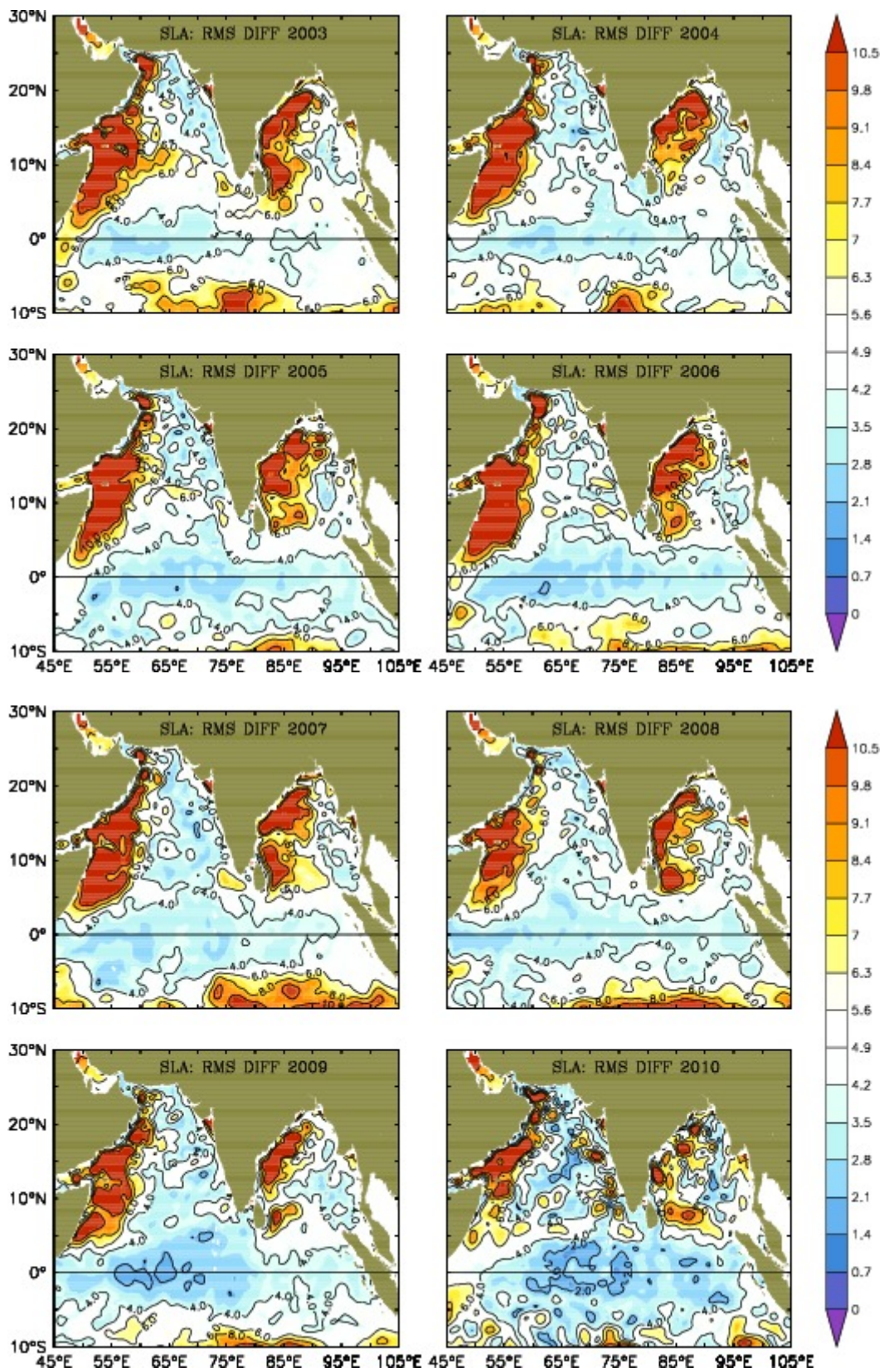


Figure 4: RMS difference between HYCOM SLA and altimeter SLA for the period 2003–2010.

corroborates, the pattern of model performance revealed in the RMS difference maps. The areas of poor correlation are the regions of both western boundaries where the non-linear dynamics is dominant in the ocean. The correlation maps from 2003 – 2010, consistently shows higher correlation between model and altimeter close to the west coast India(eastern boundaries) in Arabian sea. In case of Bay of Bengal, better correlation is found above 20°N and eastern Bay of Bengal compared to the western Bay of Bengal. In general for the analysis period, the poor correlation between model and altimeter SLA is found to be associated with small scale eddies which are not resolved by the quarter degree model. However except for the small pockets of small scale eddies both data sets shows reliable correlation on a basin scale.

Equatorial region is found to be simulated well by the model along with the eastern boundaries in the model domain evidenced by low RMS difference values and higher correlations. In order to compare and assess the differences in temporal evolution of the sea level anomalies from both model and altimeter, twelve time series locations were identified from the model domain (Figure 6), falling in Arabian Sea, Bay of Bengal and Equatorial Indian Ocean. Both altimeter and model daily averaged time series were extracted from the selected locations and presented in Figures 7 and 8. Statistical parameters described earlier (page 4) were computed between both observed and model sea level anomalies and are presented in Table - 1. It is evident from the statistics derived from the time series, that locations in Bay of Bengal shows maximum variability in sea level in both observations and model, resulting in high standard deviations in both datasets. Maximum variability in sea level is demonstrated at location AH-5 (95E:15N) which is closer to the coast, where model demonstrate a reliable skill score of 0.89 and strong correlation of 0.83 with respect to observed sea level by altimeter. The next two locations with higher standard deviations too fall in Bay of Bengal (AH-6 and AH-2). Except in the case of a coastal Arabian Sea location AH-12 (73E:15N) at all locations, model standard deviations of sea level anomalies are found to be lower than that of altimeter observed sea level anomalies. Among the selected locations, the highest RMS difference (9.52) is found to be at a coastal BoB location AH-6 (85E:18N). The central Arabian Sea location AH-7 (63E:15N) showed the poorest model skill and the coastal location AH-12 showed the highest model skill in simulating sea level.

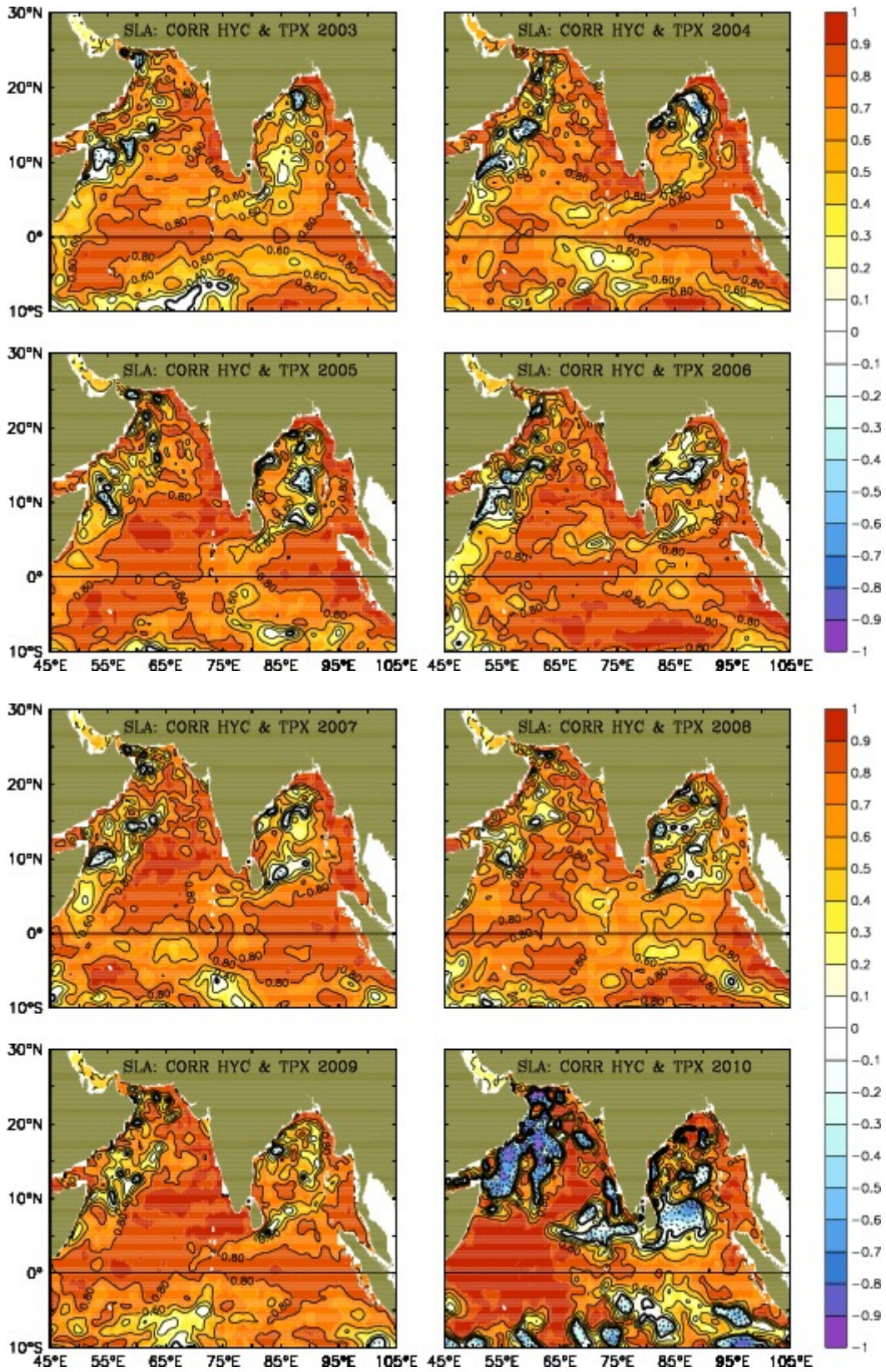


Figure 5: Correlation of HYCOM SLA with altimeter SLA for the period 2003–2010

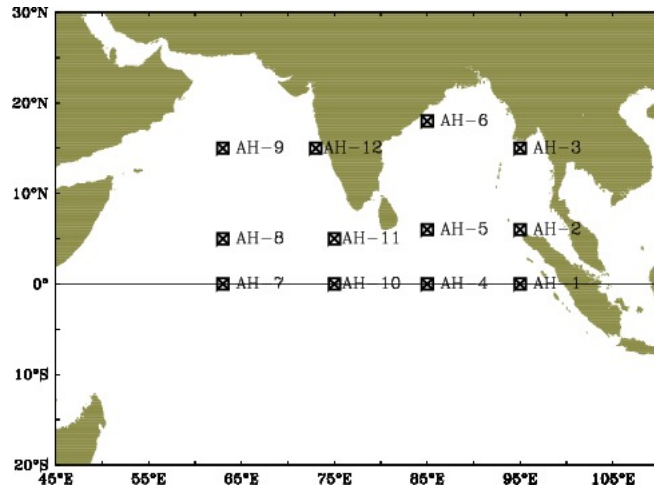


Figure 6: Selected Sample locations were daily SLA time-series where chosen for validation

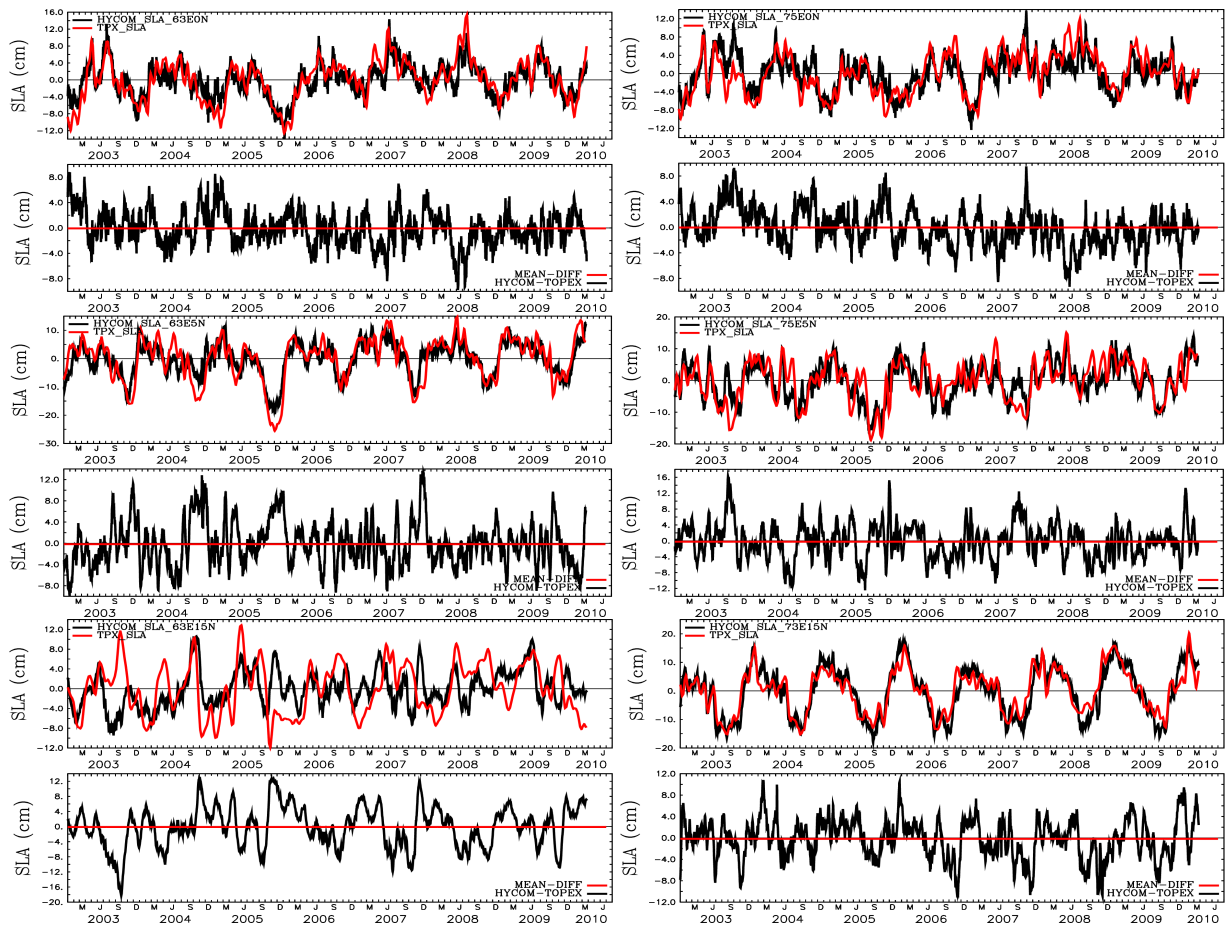


Figure 7: Comparison of HYCOM SLA with altimeter SLA time-series at Equatorial Indian Ocean and Arabian Sea locations

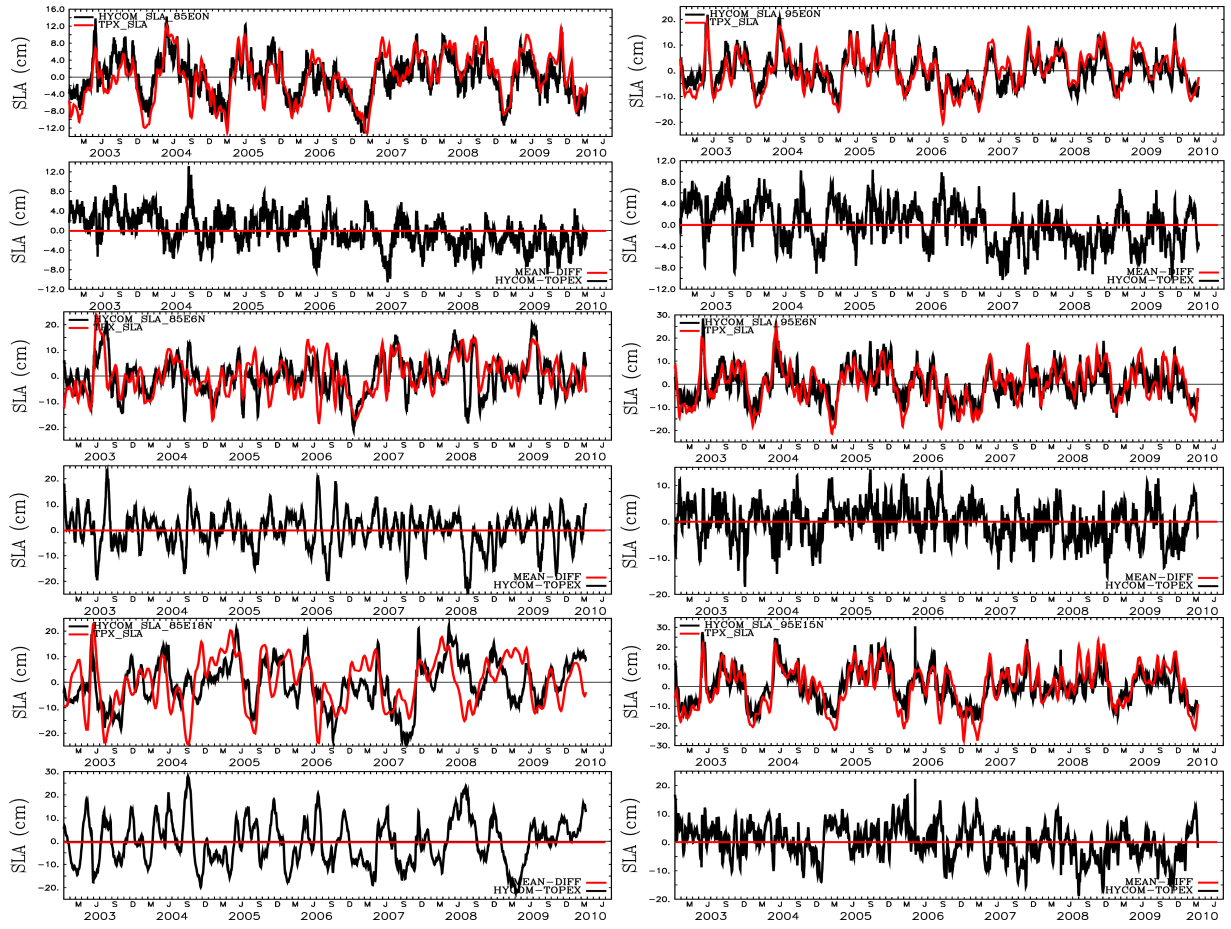


Figure 8: Comparison of HYCOM SLA with altimeter SLA time-series at Equatorial Indian Ocean and Bay of Bengal locations

LOCATION	STD-ALT	STD-HYC	RMSD	CORR	SS
AH-01(95E:00N)	7.26	6.22	3.74	0.86	0.74
AH-02 (95E:06N)	8.01	6.78	4.91	0.79	0.62
AH-03 (95E:15N)	10.58	8.36	5.87	0.83	0.69
AH-04 (85E:00N)	5.45	4.64	3.31	0.80	0.63
AH-05 (85E:06N)	7.07	6.91	6.82	0.52	0.07
AH-06 (85E:18N)	9.70	8.57	9.52	0.46	0.04
AH-07 (63E:00N)	4.79	3.90	2.71	0.83	0.68
AH-08 (63E:05N)	7.64	5.81	4.19	0.84	0.70
AH-09 (63E:15N)	5.09	3.61	5.40	0.27	-0.13
AH-10 (75E:00N)	4.36	3.88	2.88	0.76	0.56
AH-11 (75E:05N)	6.33	5.71	4.38	0.74	0.52
AH-12 (73E:15N)	7.46	8.63	3.69	0.91	0.75

Table 1: Comparison of SLA Statistics from HYCOM and altimeter at locations marked in Figure - 6

5.2 Currents

In order to assess the ability of HYCOM to capture the spatial evolution of basin scale circulation features of Indian Ocean, a monthly climatology for currents was computed using the model runs for the period 1-JAN-2003 to 31-DEC-2011. For comparison, we used the Ocean Surface Current Analyses Real Time (OSCAR) analyses, which represents the average currents from the surface to 15 m (*Bonjean and Lagerloef, 2002*) available as 5 day averages on a $1^\circ \times 1^\circ$ grid from <http://www.oscar.noaa.gov/index.html>. A climatology for the same period of model runs is calculated using OSCAR analysis also for comparison with the model currents. The monthly evolution of currents from OSCAR and the model simulation is presented in Figures- 9– 11. The dominant currents from the basin described in the literature are found to be present in the monthly climatology of both OSCAR and HYCOM. The signatures of winter monsoon starts evolving from November with development of westward currents (dominantly wind driven) Bay of Bengal, Arabian Sea and in equatorial Indian Ocean (*Shankar et al., 2002*) and is well represented in both OSCAR and model currents (Figure - 9–11). Development of Winter Monsoon Current (WMC) can be seen in both OSCAR and model during December to Feb. However though northward flowing West India Coastal Current (WICC) (JAN), southward East India Coastal Current (EICC) are present in model simulation, they are slightly less represented in OSCAR currents as OSCAR analysis is not available close to the coast. There is a dramatic reversal of currents at equator from April onwards in both OSCAR and HYCOM simulated currents, which is well documented and is associated with the seasonal monsoon circulation pattern in the basin. In April, the development of Wyrтки jets can be seen in both OSCAR and model currents. By May, the WMC reverses direction to become Summer Monsoon current (SMC) and is well represented in both OSCAR and model results. The Wyrтки Jets get matured in both OSCAR and model solutions by May, and starts dissipation from June to July. However the HYCOM solution is showing slightly higher speeds and narrower jets than the OSCAR analysis, which is anticipated given the much higher model resolution (Figure 9–11). From September the Wyrтки Jets starts re appearing in both OSCAR and model currents and become matured by November. Starting from May, in both OSCAR and model solutions, the northward flowing WICC reversed direction towards south and EICC became northward, which is in agreement with the descriptions in literature *Shankar et al. (2002)*.

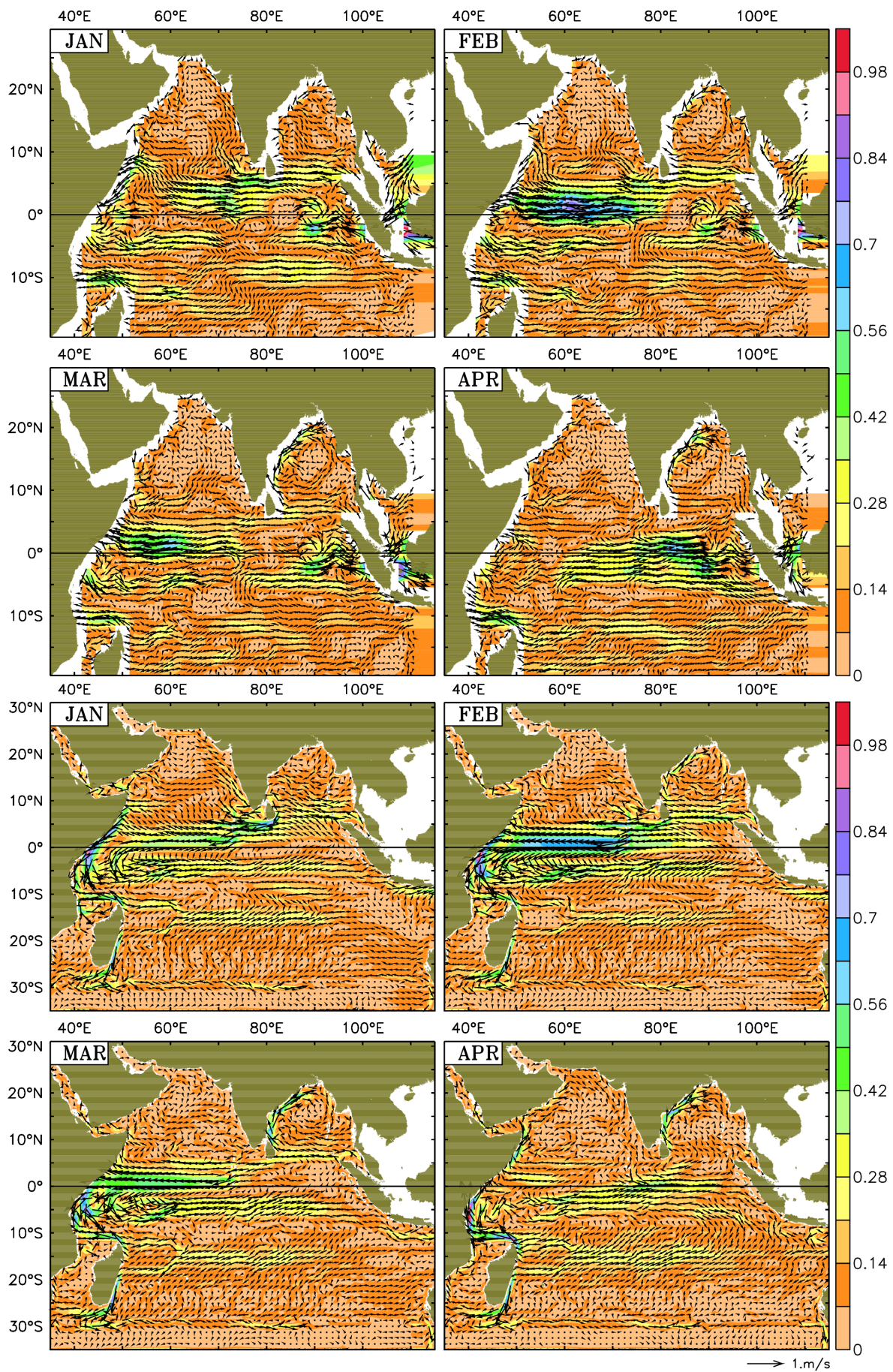


Figure 9: Evolution of OSCAR (top) and model (bottom) currents during January to April

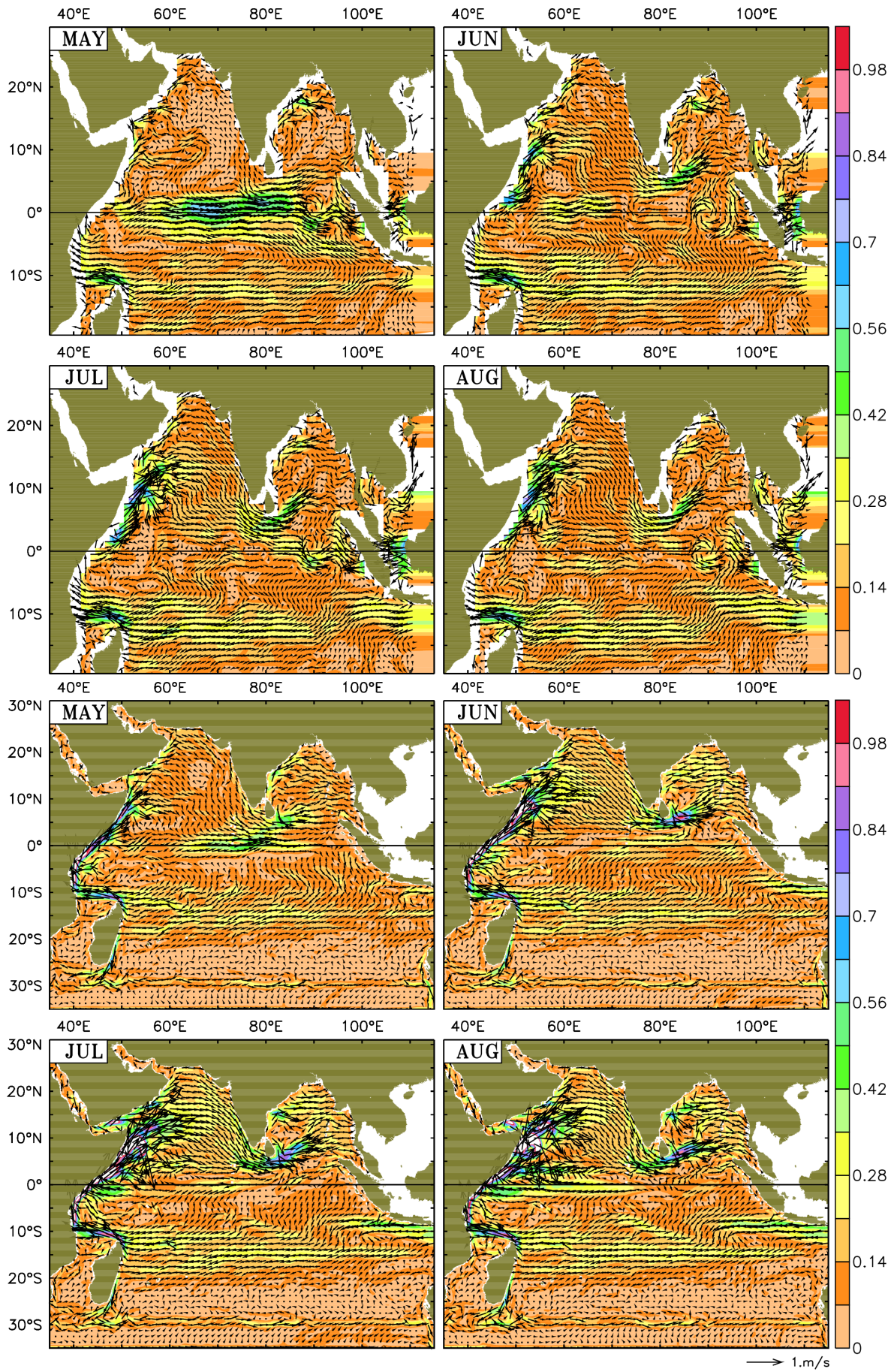


Figure 10: Evolution of OSCAR (top) and HYCOM (bottom) currents during May to August

Another well known feature of Indian Ocean circulation present in the OSCAR and model simulation is the western boundary current (Somali Current)(SC), which reverses direction in resonance with the monsoon related atmospheric forcing. From December to February SC is flows towards south and from May it reverse to a northward flow along the western boundary. At the western boundary of the basin two associated persistent eddy fields, the Great Whirl (GW) and the Socotra Eddy (SE) are present which are described in literature (*Bruce, 1970, 1979*). Both these eddy fields observed to be evolving from June onwards in both OSCAR and Model solutions and reaching their peak intensity in August and seen as dissipating from September onwards. However the HYCOM solution provides a better representation as OSCAR is not computed close to the coast. South Equatorial Current (SEC) is a dominant feature of the southern tropical Indian Ocean (*Cutler and Swallow, 1984; Shenoi et al., 1999; Schott and McCreary, 2001*) which show its clear presence in both OSCAR and model fields. It is the strongest permanent current and is always found within 8°S-20°S. During the SW monsoon, the strength of the SEC increases and it separates into southward and northward branches near the coast of Africa (Figure - 10). The northward branch joins the East African Coastal Current (EACC) and becomes part of the basin-wide gyre along with the South Equatorial Counter-current (SECC). The SEC and SECC are described as currents that show annual variations without a reversal (*Donguy and Meyers, 1995*).

For comparing daily mean currents from HYCOM, daily mean currents from Research Moored Array for African–Asian–Australian Monsoon Analysis and Prediction (RAMA) array of buoys were used. HYCOM currents from the quarter degree resolution model were interpolated to the location of the buoys. Though there is a possibility of mismatch between quarter degree resolution model and point observation of currents by moored buoys due to scale difference itself, we use these buoys to validate the model currents due to the lack of other reliable current data with similar resolution. Figure- 12 present the locations of the selected (based on availability of longer time-series) RAMA buoys with current measurements. From the selected RAMA buoys, the daily averages of zonal and meridional components of the currents were computed and were compared against daily averaged model outputs samples at the same depth (10 m),location and time. As the current data quality may vary depended on sensor stability and environmental conditions, the quality flags were also plotted so that the comparison can be better evaluated. The graphics of quality flags of each buoy compared and the description of each of the quality flags ranging

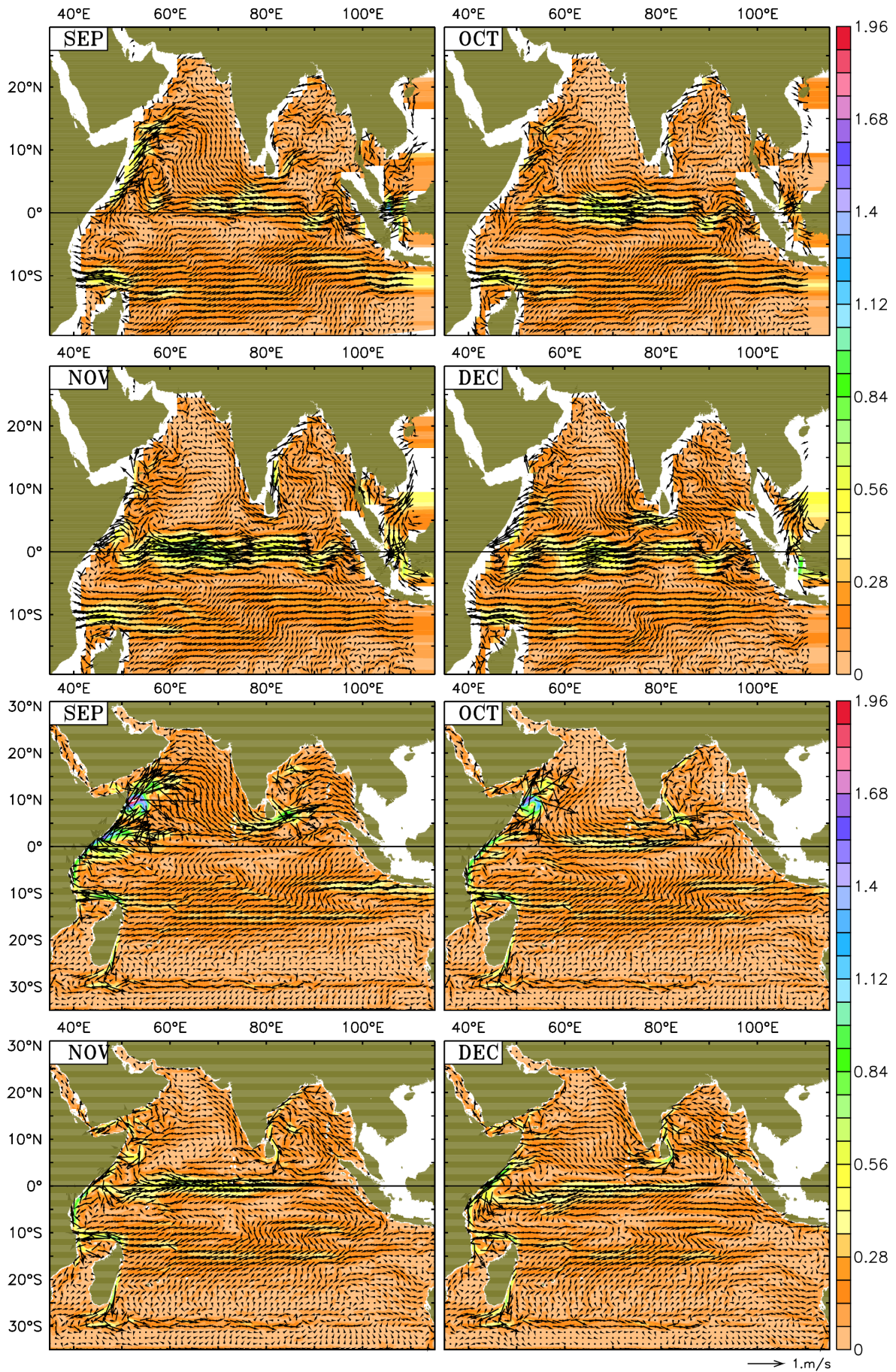


Figure 11: Evolution of OSCAR (top) and HYCOM (bottom) currents during September to December

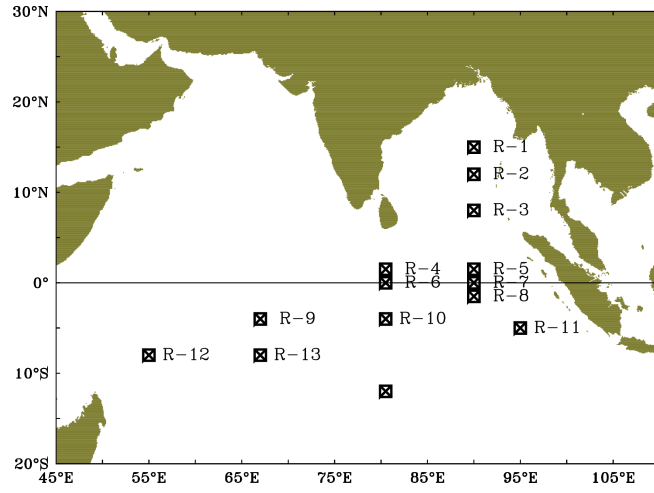


Figure 12: Location of RAMA buoys selected for comparison of Currents and calculating statistics

LOCATION	$R\bar{U}$ m/s	$H\bar{U}$ m/s	STD-RU	STD-HU	RMSD	CORR	SS
R01(90.0E:15.0N)	0.03	0.06	0.19	0.15	0.18	0.40	-0.00
R02(90.0E:12.0N)	0.04	-0.05	0.18	0.13	0.19	0.21	-0.40
R03(90.0E:8.0N)	0.03	-0.01	0.17	0.17	0.17	0.49	-0.10
R04(80.5E:1.5N)	0.13	0.02	0.40	0.37	0.24	0.79	0.52
R05(90.0E:1.5N)	0.07	0.04	0.35	0.32	0.29	0.62	0.29
R06(80.5E:0.0N)	0.23	0.17	0.47	0.46	0.24	0.85	0.68
R07(90.0E:0.0N)	0.06	0.00	0.38	0.36	0.27	0.73	0.46
R08(90.0E:1.5S)	-0.01	-0.01	0.32	0.33	0.24	0.71	0.40
R09(67.0E:4.0S)	0.15	-0.01	0.16	0.16	0.10	0.76	-0.40
R10(80.5E:4.0S)	0.15	0.05	0.27	0.25	0.18	0.73	0.34
R11(95.0E:5.0S)	0.08	0.09	0.19	0.21	0.20	0.50	-0.10
R12(55.0E:8.0S)	-0.04	0.15	0.20	0.25	0.20	0.60	-0.90
R13(67.0E:8.0S)	-0.03	-0.05	0.14	0.19	0.19	0.39	-0.70
R14(80.5E:12.0S)	-0.17	-0.07	0.20	0.16	0.20	0.35	-0.30

Table 2: Statistics of Rama buoy Zonal current velocities and same simulated by HYCOM extracted at same time and space.

LOCATION	$R\bar{V}$ m/s	$H\bar{V}$ m/s	STD-RV	STD-HV	RMSD	CORR	SS
R01(90.0E:15.0N)	0.03	-0.01	0.21	0.13	0.21	0.22	-0.10
R02(90.0E:12.0N)	0.05	0.13	0.15	0.12	0.20	-0.00	-0.90
R03(90.0E:8.0N)	0.03	0.04	0.16	0.15	0.20	0.18	-0.50
R04(80.5E:1.5N)	-0.02	0.00	0.21	0.18	0.18	0.56	0.21
R05(90.0E:1.5N)	0.02	0.03	0.23	0.21	0.20	0.58	0.21
R06(80.5E:0.0N)	0.01	0.04	0.22	0.19	0.18	0.57	0.21
R07(90.0E:0.0N)	-0.03	-0.00	0.21	0.21	0.19	0.55	0.09
R08(90.0E:1.5S)	-0.05	-0.04	0.23	0.23	0.22	0.52	0.03
R09(67.0E:4.0S)	-0.04	-0.01	0.16	0.15	0.10	0.76	0.51
R10(80.5E:4.0S)	-0.01	-0.03	0.20	0.18	0.16	0.64	0.33
R11(95.0E:5.0S)	-0.06	-0.10	0.15	0.16	0.19	0.22	-0.70
R12(55.0E:8.0S)	-0.02	-0.02	0.15	0.14	0.15	0.45	-0.00
R13(67.0E:8.0S)	-0.02	-0.02	0.15	0.17	0.11	0.41	-0.30
R14(80.5E:12.0S)	-0.06	-0.09	0.12	0.11	0.11	0.45	-0.00

Table 3: Statistics of Rama buoy meridional current velocities and same simulated by HYCOM extracted at same time and space.

from 0 to 5 is presented in Appendix-I. In general the statistics are better in areas of strong persistent currents. Current comparisons are found to be better in the equatorial belt where the magnitude of currents are rather high and the model demonstrates better skill in reproducing the same.

In case of Bay of Bengal 15°N site R-01, both observed and model currents shows a seasonal amplification in eastward amplitude in case of zonal currents starting from June and reaching minimum by end of September (Figure - 13, top left panel). This cannot be verified at site R-02 as data gaps are more at this site. However at both site R-01 and 12°N site (R-02) the mean zonal and meridional currents are relatively weak in case of both observed and modeled currents (Table- 2 & 3). The RMS difference between model and observed currents at R-01 is 0.18 m which is less than the standard deviation of the observed currents (0.19 m). Though the mean model current is higher than that of the observed currents, model standard deviation is lower compared to the observed variability. Thus the statistical parameters indicate that the model is not reproducing the full spectrum of variability present in the observed currents using the given forcing and configuration and thus resulting in poor skill scores. Similar is the case of the location R-03 resulting in poor skill score. However in case of site R-03 the zonal currents show relatively better correlation with the observed currents (Figure - 12, 13, Table - 3). In case of site R-03 too a low amplitude seasonal cycle with long wave length can be observed in case of both observed and model currents. But as comparisons get closer to the equator, where the measurements are from persistent and relatively strong

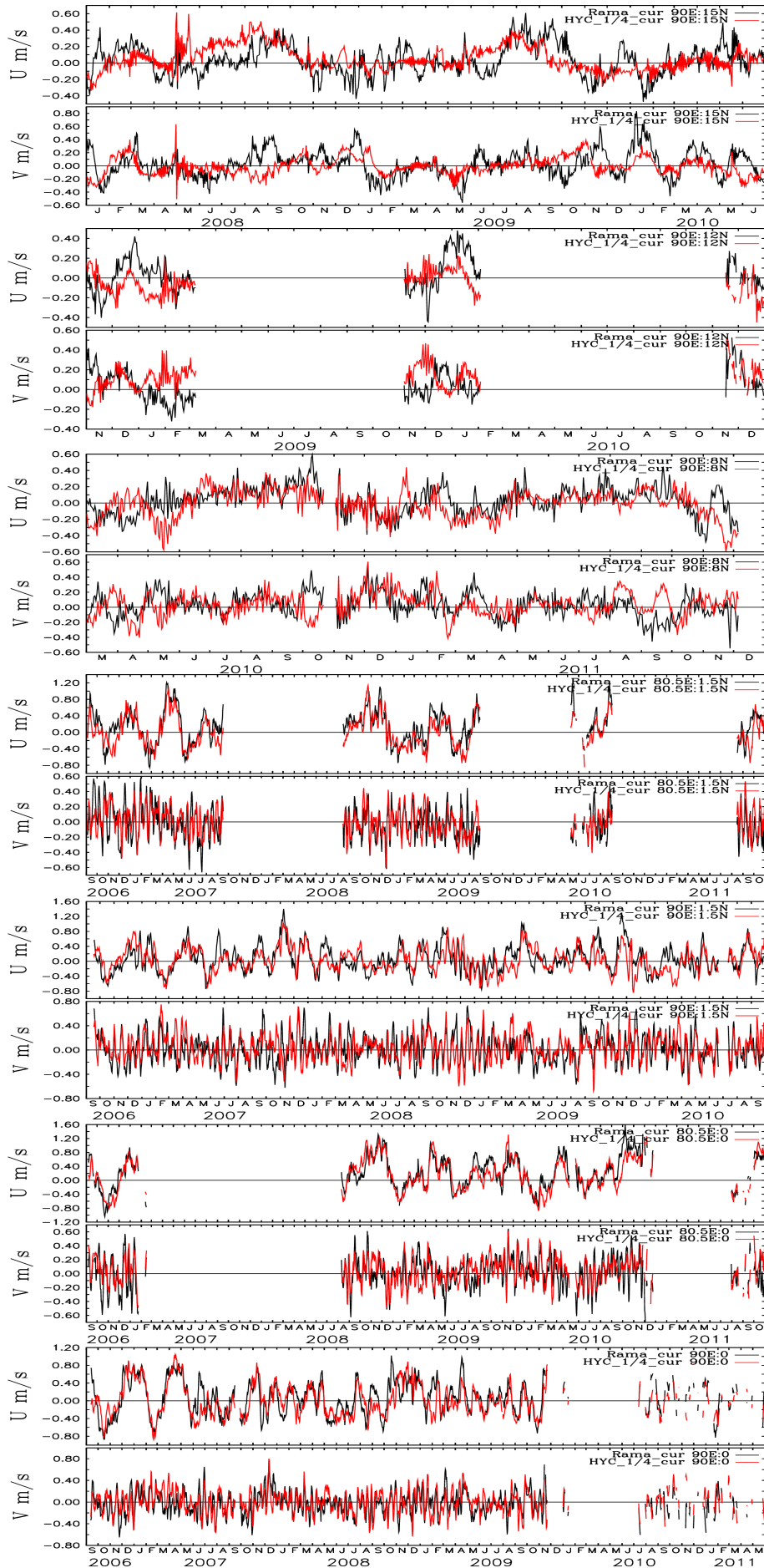


Figure 13: RAMA-BUOYS selected for comparison of Currents and calculating statistics in equatorial Indian Ocean locations

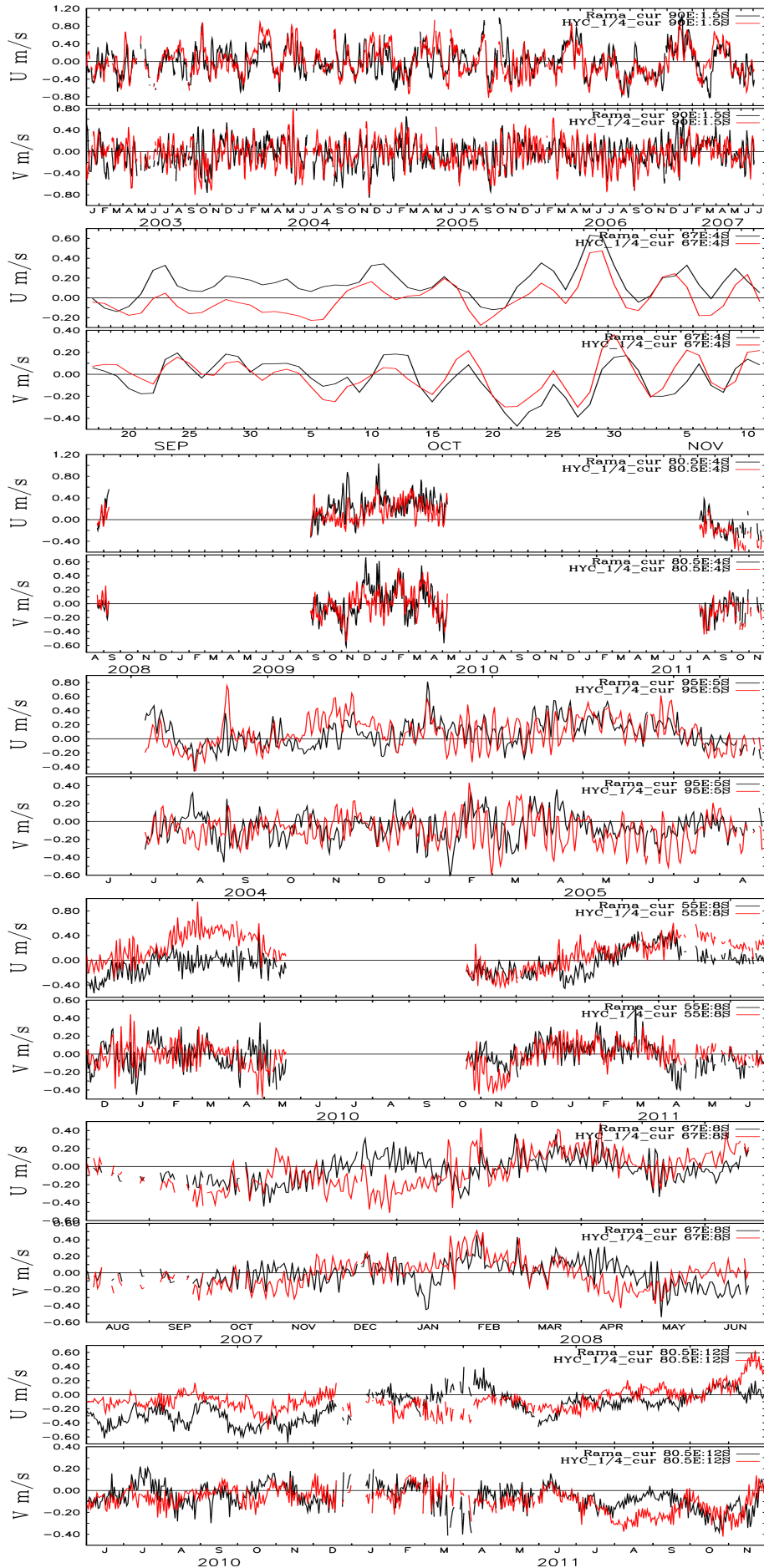


Figure 14: RAMA-BUOYS selected for comparison of Currents and calculating statistics in equatorial Indian Ocean locations

currents, the model skill and correlations show dramatic improvements as evident from Figure- 13 & 14 and Table - 2 & 3 particularly in case of zonal velocities. As the meridional velocities remains smaller at equator the improvements in case of it is not as dramatic as that of zonal currents. As the samples get closer to the equator the low frequency reversals of zonal currents seen at northern locations are replaced by more sharp and high frequency reversals with higher amplitudes.

In case of southern Indian Ocean moorings, mooring site R-09 at 67E-4S location shows a relatively strong correlation of 0.76 rms difference of 0.10m/s, with a relatively good skill of 0.51. The correlation is particularly poor in case of site R-11 at 95E-5S where the model may have influence of relaxation at eastern boundary.

5.3 Sea Surface Temperature (SST)

The ability of HYCOM to reproduce the SST pattern in basin scale is assessed using TMI SST gridded to the same grid size of model and by computing the Root Mean Square Difference (RMSD) (Figure - 16) and correlation (Figure - 17) between the 2 data set for the period 2003 to 2010. For year 2003 for most of the areas close to the Indian east coast and west coast have a minimum RMSD falling between 0.25 to 0.5. However the western part of Arabian Sea and eastern part of Bay of Bengal has RMS difference raging from 0.5 to 0.75. Also there are small patches of high RMS differences close to the east African coast. Another area with poor SST simulation from the model is close to the eastern equatorial Indian Ocean where the RMSD goes above 1°C . Correlation (Figure - 16) for the Arabian Sea and Bay of Bengal falls above 0.9 except for pockets where it goes to the range 0.8 – 0.9. At around 85°E and 5°S , there is a small pocket where the correlation goes poor though the RMSD remains less than 0.5°C . This could be a region with low amplitude SST variability which may have resulted in good RMS score and poor correlation. During 2004 the pattern of RMSD is almost similar but the area of poor correlation in the eastern Indian Ocean become more intense which may be attributed to inter annual variability influenced by the relaxation in the eastern model boundary where intra-basin transports get affected due to relaxation to climatology. The examination of correlation for 2004 (Figure - 16) indicate, such possibility as eastern Indian Ocean has a poor correlation to the observed SST during 2004 indicating some part of the total spectrum of oceanic SST variability is not captured fully by model. In 2005 the area of high RMSD in the eastern Indian Ocean get reduced and the pattern

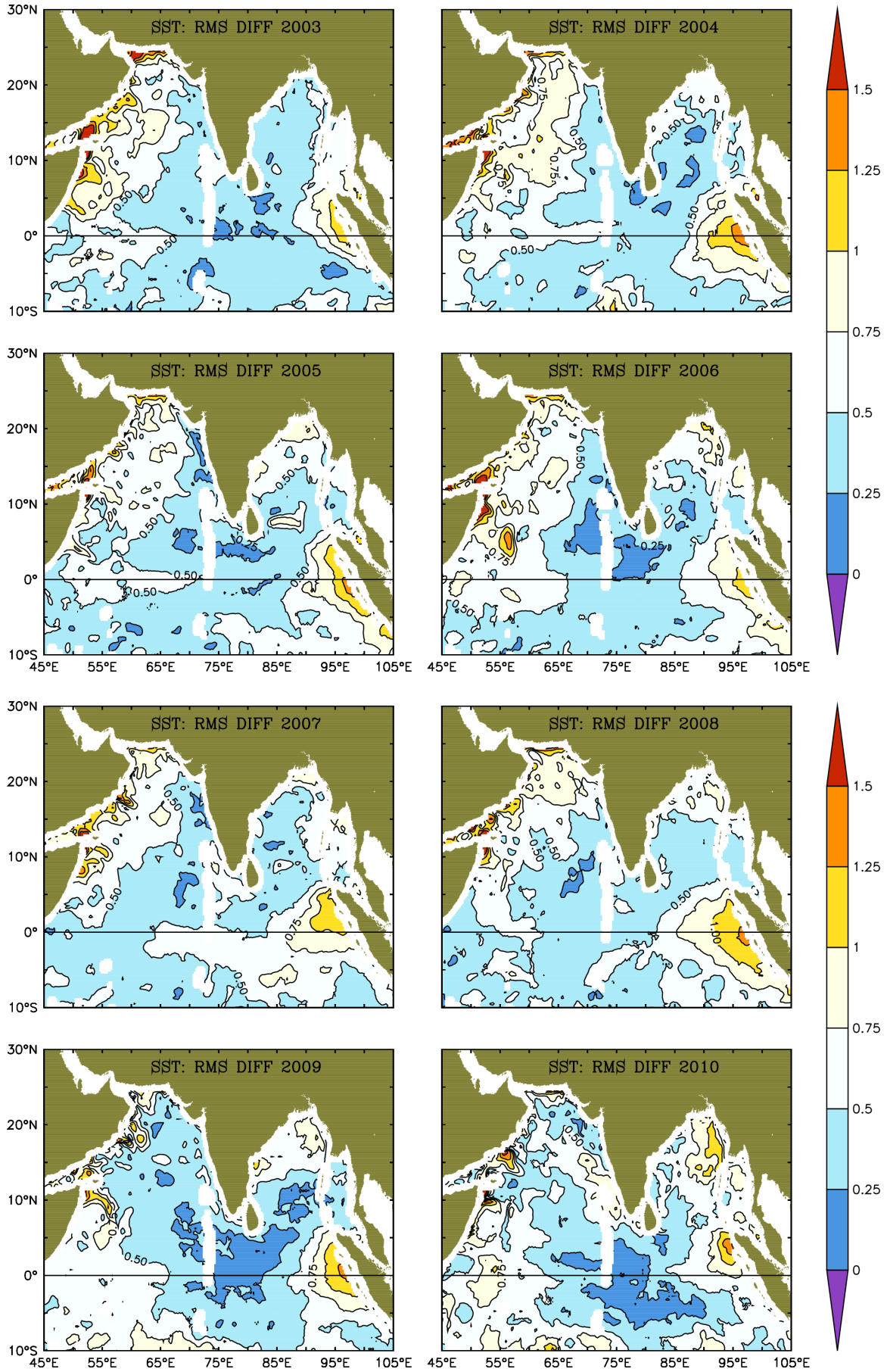


Figure 15: HYCOM SST RMS difference with TMI SST

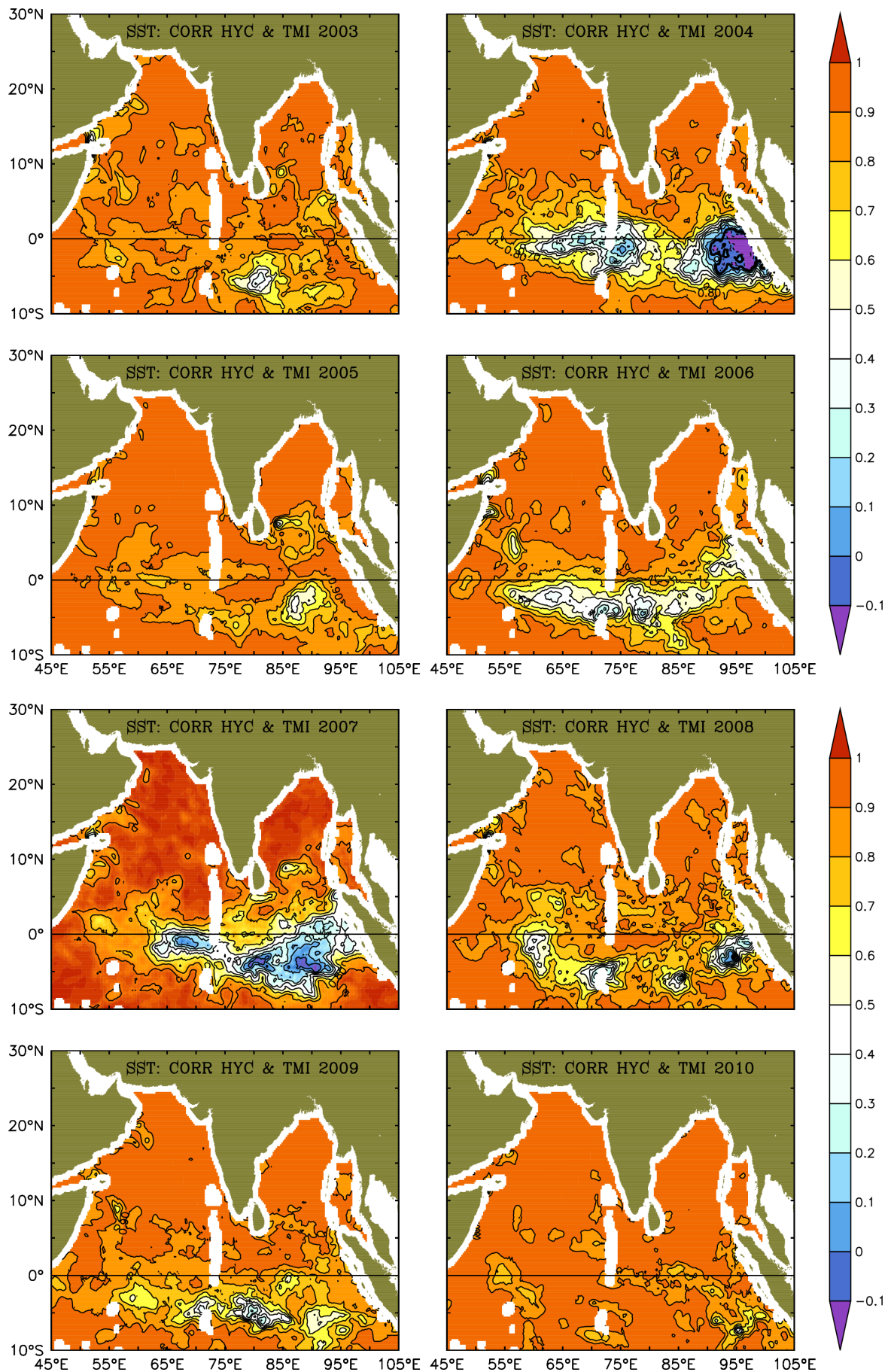


Figure 16: HYCOM SST Correlation with TMI SST

goes back close to the one in 2003 (Figure - 15) . The correlation remains above 0.9 for most of the basin except for small patches and a notable low correlation area in south eastern Indian Ocean (Figure - 16). In 2006 there is a small patch of large RMSD appears in western Indian Ocean close to the Great whirl (Figure - 15). In northern Bay of Bengal too the SST comparison go slightly poor during 2006. However the correlation remains above 0.9 during 2006 in both the above areas indicating the lower RMSD could be due to a bias in the model with respect to TMI SST for this period rather than the model deficiency in capturing all scales of variability during this time. Across the longitudes there is a relatively large patch of poor correlation just south of equator during 2006 with lower RMSD indicating low amplitude variability poorly captured by model (Figure - 15). During 2007 and 2008 the eastern Indian Ocean patch of poor SST simulation (high RMSD) remains above 1°C , which may have been partly induced by the poor representation of intra-basin large scale processes like Indian Ocean dipole and ENSO and related oceanic exchanges due to the relaxation in the eastern boundary. This is also supported by the poor correlation between the observed and modeled SST in this area (Figure - 16). During 2009 the large part of Arabian sea shows a better simulation of SST compared to other years and Bay of Bengal becoming slightly poor in simulation. Both Arabian Sea and Bay of Bengal shows correlation above 0.9. However the patch of poor correlation south of equator remains there. During 2010, the central part of Arabian sea became slightly poor along with eastern Bay of Bengal. However the correlation remains high through out the basin indicating that the high RMSD of the model with observation is due to bias induced by atmospheric fluxes rather than models deficiency in capturing variability. The temporal evolution of SST from model is assessed by comparing with observed time series of RAMA buoy SST at 14 locations with long time series sampled at same day and location (Figure - 18). The locations of the selected Rama buoys are presented in Figure - 17. The statistics of the SST comparison of model with that of RAMA buoys is presented in terms of MEAN (\overline{RSST} \overline{HSST}), Standard deviation (STD-RSST, STD-HSST), Root Mean Square Difference (RMSD), Correlation(COR), and SKILL in Table - 4. At the northern most location (Figure - 17, R-01) of RAMA buoy SST and model SST demonstrate a reasonably good agreement (Figure - 18,col-1,row-2). Both RAMA and HYCOM SST shows a comparable standard deviation of 1.08°C and 1.23°C each with RMSD of just 0.32°C . Model shows a skill of 0.69 in reproducing SST observed by RAMA. Both observations and model shows a dominant annual cycle at this location with an SST minimum in

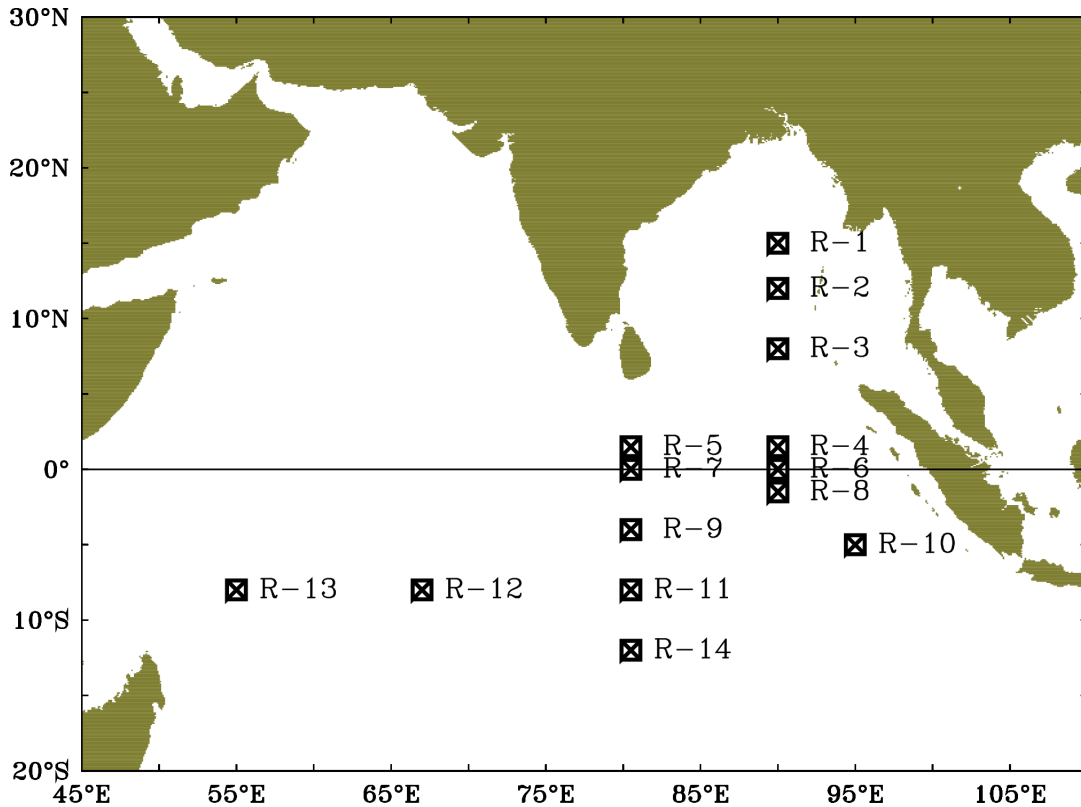


Figure 17: Location map for RAMA buoys used for SST validation

December–January–February months. The seasonal cycle is observed to be embedded in the large amplitude annual cycle. As the sample location shifts to location R-02 at 12°N, the seasonal cycle become more evident with appearance of distinct peaks during April–May and October along with the SST minimum of winter (Figure - 18, col-1,row-2). In both the above locations, the 2010 SST maximum during May is anomalously high in comparison with other years for both observation and model. The RAMA model comparison gives a relatively better correlation of 0.92 at the location R-02 and higher skill of 0.77. At location R-03 at 8°N , both model and RAMA SST shows dominant seasonal cycle relative to the annual cycle which was prevalent at two northern locations described above. Here both the observed and model mean SST are closer 28.8°C and 28.58 °C each. Standard deviations reduced to 0.62°C and 0.70°C respectively. RMS difference is 0.17°C . The correlation and skill are some what lower than the 2 northern location which may be attributed to the reduced range of variability of SST indicated by the lower standard deviations. At the location R-04, the SST of both RAMA and model shows an increase in mean reaching 29.29 and 29.22 respectively. At this location, the variability of SST is observed to be low for both RAMA and HYCOM, and their standard deviations are comparable (Figure - 18 and Table - 4). However the RMSD is much less (0.21) than the standard deviations. As the range

LOCATION	RSST	HSST	STD-RSST	STD-HSST	RMSD	COR	SKILL
R01(90.0E:15.0N)	28.77	28.62	1.08	1.23	0.32	0.88	0.69
R02(90.0E:12.0N)	28.90	28.66	0.99	1.04	0.16	0.92	0.77
R03(90.0E:08.0N)	28.86	28.58	0.62	0.70	0.17	0.81	0.35
R04(90.0E:01.5N)	29.29	29.22	0.55	0.51	0.20	0.64	0.31
R05(80.5E:01.5N)	29.16	28.68	0.53	0.45	0.18	0.62	-0.48
R06(90.0E:00.0N)	29.29	29.13	0.57	0.51	0.25	0.56	0.13
R07(80.5E:00.0N)	29.30	28.69	0.56	0.50	0.18	0.68	-0.81
R08(90.0E:01.5S)	29.28	29.03	0.56	0.46	0.27	0.48	-0.09
R09(80.5E:04.0S)	28.95	28.49	0.62	0.45	0.15	0.77	0.04
R10(95.0E:05.0S)	28.97	28.75	0.68	0.63	0.21	0.75	0.43
R11(80.5E:08.0S)	28.27	27.69	0.73	0.74	0.24	0.77	-0.11
R12(67.0E:08.0S)	28.33	27.43	0.91	0.77	0.32	0.78	-0.39
R13(55.0E:08.0S)	28.10	27.12	1.19	0.89	0.42	0.84	0.01
R14(80.5E:12.0S)	27.10	26.33	0.93	0.82	0.32	0.79	-0.07

Table 4: Statistics of Rama buoy SST and same simulated by HYCOM extracted at same time and space.

of variability in SST is much reduced, the correlation and SKILL values are relatively small compared to the northern locations. The pattern of SST behavior at equatorial locations R-05 to R-08 is almost same as that of R-04 indicating similar behavior at the equatorial belt. For the location R-09 at 4°S, there is again an increase in standard deviation of SST in both observation and model resulting in improved correlation and better skill. The model skill shows further improvement at R-10 at 5°S with skill value reaching 0.43. For the further south locations R11-R14 the standard deviations from both RAMA and model are somewhat higher. However standard deviations are less than 1°C for southern sites except for R-13 where both correlation and skill is better relatively better, though for all these locations, the correlation is ≥ 0.75 . However in general the model skill is poor for the southern locations which may be due to the influence of climatological relaxation at the eastern boundary. Here the natural exchanges between the Pacific and Indian Ocean basins are limited only through atmospheric fluxes. The analysis of SST from RAMA moorings in comparison with HYCOM reveals a systematic pattern of model behavior with respect to the location of sampling. In general the northern and southern locations show relatively larger variability and lower mean values, the correlation and skill at these locations are relatively high. As the sampling locations move close to the equator the SST variability gets reduced and the mean SST values go up in both model and observations. At these equatorial locations the correlation and skill becomes relatively poor.

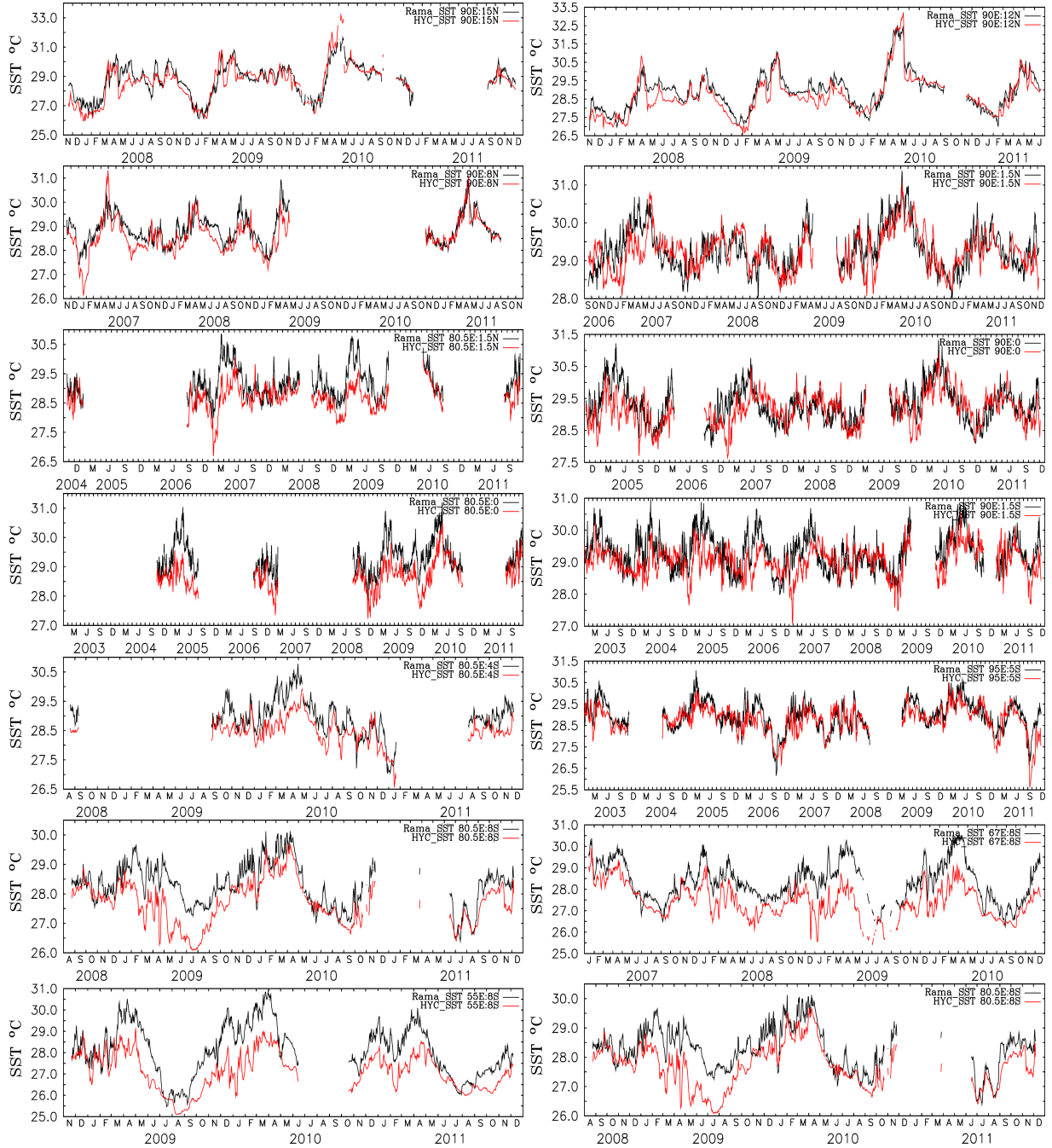


Figure 18: Comparison of SST from selected RAMA-BUOYS and HYCOM SST interpolated to the location of each. Corresponding statistics are presented in Table - 4

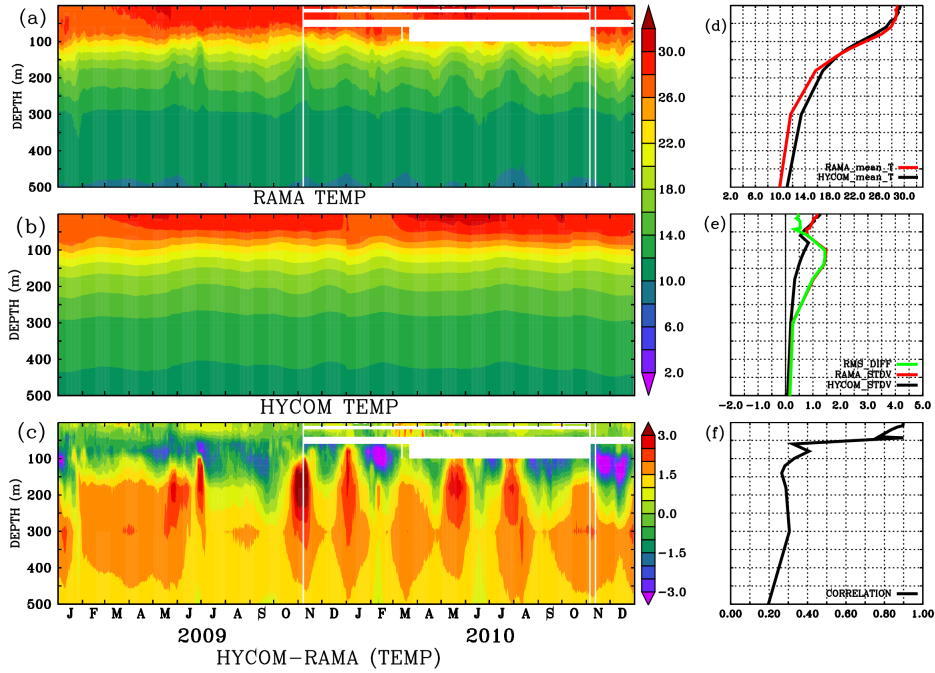


Figure 19: Time depth section of RAMA mooring at 90°E 15°N compared against HYCOM temperature sampled at same location.

5.4 Vertical Profiles of Temperature

Vertical profiles of temperature from HYCOM is validated using temperature sampled by selected RAMA buoys with long time series particularly for Bay of Bengal region from 15°N to equator and also using selected ARGO float observations for other regions. The model equivalents of time depth sections of RAMA and ARGO are obtained from HYCOM simulated temperature by sampling the model grid at same time and location where the observation platform sampled the ocean. For computing the statistics, the gaps in sampling are artificially imposed in model time depth sections. The statistics are presented in graphs. Apart from this, 181 Argo floats selected from Indian Ocean are used for computing statistics and is made available on line at INCOIS web site (http://www.incois.gov.in/HYCOM/HA_tempz/node1.html)

At the 15°N 90°E RAMA buoy obtained temperature profiles continuously for 2 years starting from January 2009, with three short gaps in between for the full vertical column. But there is a long window of bad sampling evident from data gaps above 100 meters starting from November 2009 continuing till the end of 2010. However this buoy provides an opportunity to compare the vertical thermal structure of the ocean at this location with that simulated by HYCOM. Comparison of time depth section of temperature profiles from RAMA (Figure - 19 a,b), reveals that there is a good amount of seasonal variability in thermal structure at this

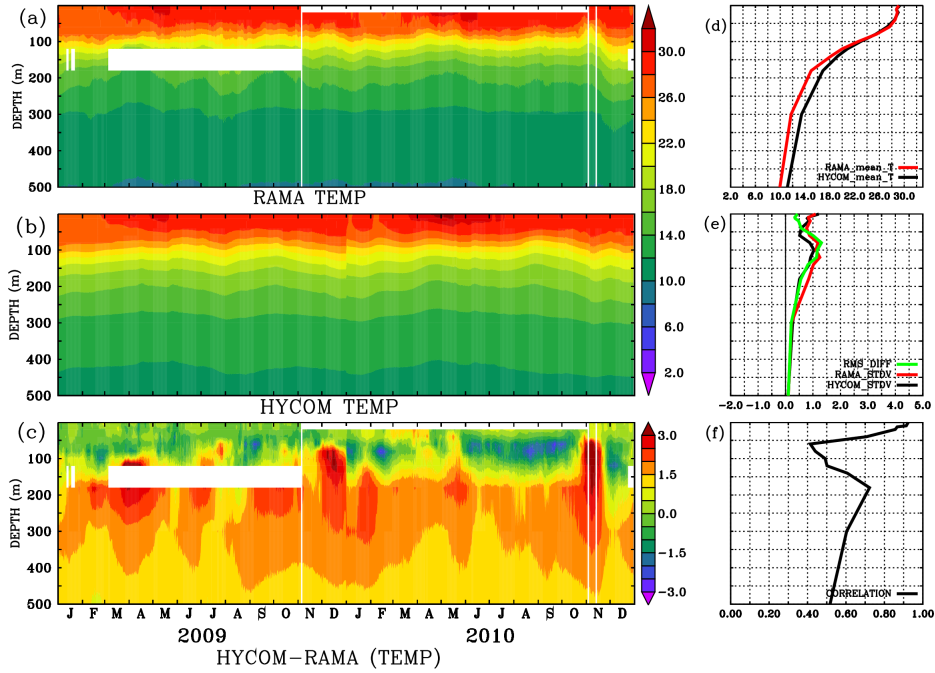


Figure 20: Time depth section of RAMA mooring at 90° E 12° N compared against HYCOM temperature sampled at same location

location even up to deep layers of 300 m depth, both in Argo and HYCOM sections. However there are subtle differences in the representation of these variability in observation and model. In case of RAMA, the thermal contours shows sharp kinks whereas the model represents these variabilities in a more smoothed manner. In case of RAMA temperature section, there is an anomalous upward trend in thermal contours clearly seen from about 300 m depth up to 100 meters on either side of the small data gap before November 2009 which is apparently an artifact in RAMA data due to sensor issues resulting in relatively large red patch difference plot in lower left panel close to the data gap. There are also large patches of differences just before and below the data gap. In spite of the differences, the mean profiles from both RAMA and HYCOM are close to each other as evident from the panel d of Figure - 20. The standard deviation from both data sets are closer to each other (Figure - 20, e) and the RMSD are close to the standard deviation for the subsurface and lower than it close to surface. The correlation is above .5 from 200 m depth to surface and the poor correlation for the lower part may be associated with lower scale of variabilities to which model may not be sensitive enough. From 50 meters to surface there is a correlation above 0.8 between observation and model which reaches maximum at surface with respect to SST.

At the 12° N 90° E location also the time depth section of RAMA temperature is available for a period from January 2009 to December 2010

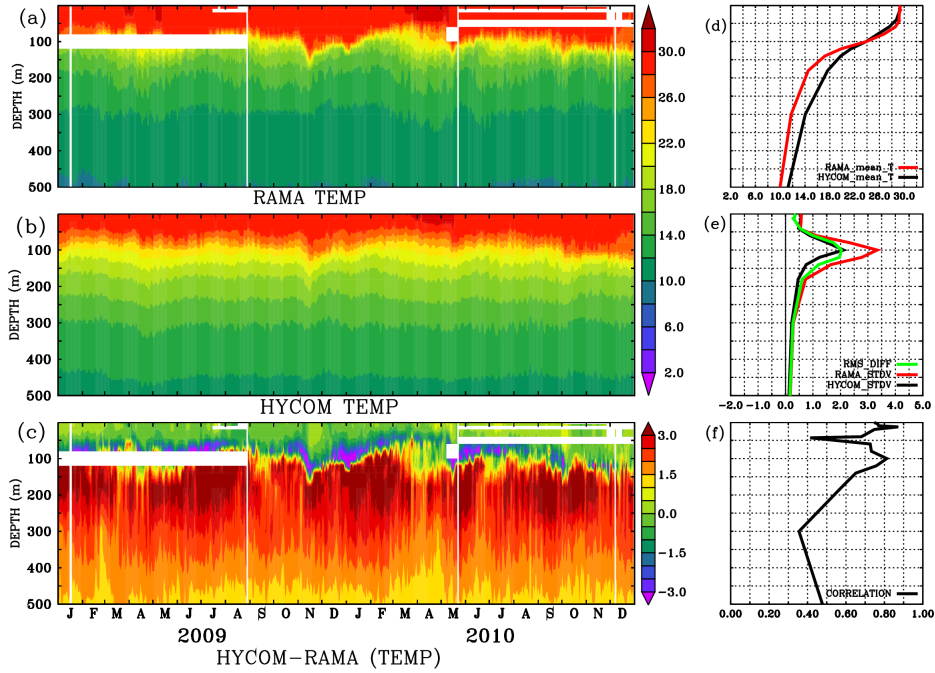


Figure 21: Time depth section of RAMA mooring at 80.5° E 0° N compared against HYCOM temperature sampled at same location

(Figure - 20). At this location, there is a vertical data gap from March to November in 2009 and the top samples are missing from November 2009 to November 2010. there are also three full profile temporal gaps close to November 2009, and November 2010. The patches with errors at thermocline are relatively less intense at this location. However there is a patch of relatively high bias close to the 2 temporal gaps which are present in November 2010. A warm bias is also observed close to 150 meters which is found to be close to the bad data occurrence in RAMA during December 2010. The standard deviations from both RAMA and HYCOM matches to a good extend and RMSD is less than both close to the surface. The correlation in vertical shows a rapid decline close to 0.4 at about 100 meter depth and restore back to above 0.7 at 150 meters. It shows a gradual decline as downwards up to 500 meter depth which is a result of poor model performance at very low variability in oceanic temperature which is less than 0.25 degree below 300 meters.

At 80.5° , on equator too, there is a 2 year temperature time series available from RAMA buoy, which is compared against the HYCOM simulated thermal field. Compared to the previous two northern sites, here the temperature contours from both observation and model shows very high frequency variability (Figure - 21). These high frequency variability is seen as deep as 500 meter which may be imparted by the subsurface currents associated with the equatorial circulation cell. A notable synergy is exhib-

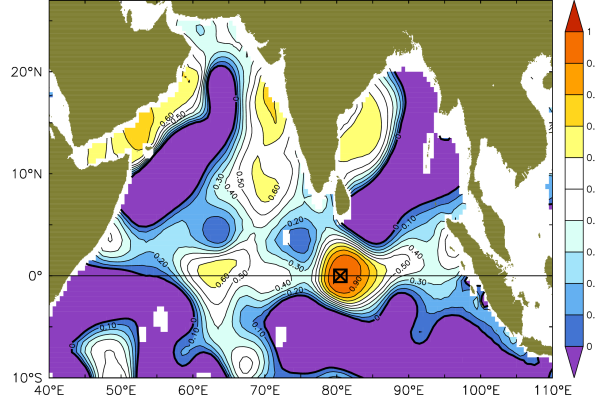


Figure 22: Spatial correlation scale of temperature at a depth of 200 m at 80.5° E 0° N

ited by model during November 2009 in capturing the sharp thermocline deepening exhibited by the measured temperatures of RAMA buoy (Figure - 21). Compared to the other 2 northern sites, the mean profile from model and RAMA are showing larger differences, particularly at around 200 m which could be due to the highly dynamic nature of oceanic processes at equator. The observed standard deviation is reaching a peak value of 3.5°C at 100 meter depth which is much higher than the model standard deviation ($\approx 2^\circ\text{C}$) and the RMSD at this depth ($\approx 2^\circ\text{C}$). The standard deviation of both model and RAMA goes below 0.5 degree for depths below 300 meters. The vertical structure of correlation shows 3 regions of sharp variations in the upper 200 meter showing deviations from 0.4 to 0.89 in the upper 100 meter and remains close to 0.4 degree at deeper layers where the standard deviations move to lower values. As the deep layers of the model were showing larger difference compared to the other northern sites, (Figure - 21 (c)), we decided to carry out a spatial correlation analysis at this location using ARGO girded temperature field. The spatial correlation analysis for year 2005 (Figure- 22) reveals that the spatial correlation at this location is very localized and is falling in the range of 0.8 within very short distance from location of RAMA buoy. This demonstrates that the spatial distance of model grid to the point observation location itself may explain about 46% loss of variance. (% Variance explained = $R^2 \times 100$)

Apart from RAMA buoys, Argo floats were chosen for validation of HYCOM vertical thermal structure for areas where RAMA buoys are not available for measuring single location time series. However, unlike RAMA, in case of ARGO floats, the profiles are with both varying time as well as location and the samples are obtained in similar way from the HYCOM simulated temperature field. For Northern Arabian Sea, Argo float NO: 2900556 was selected for assessing the model performance. Time depth

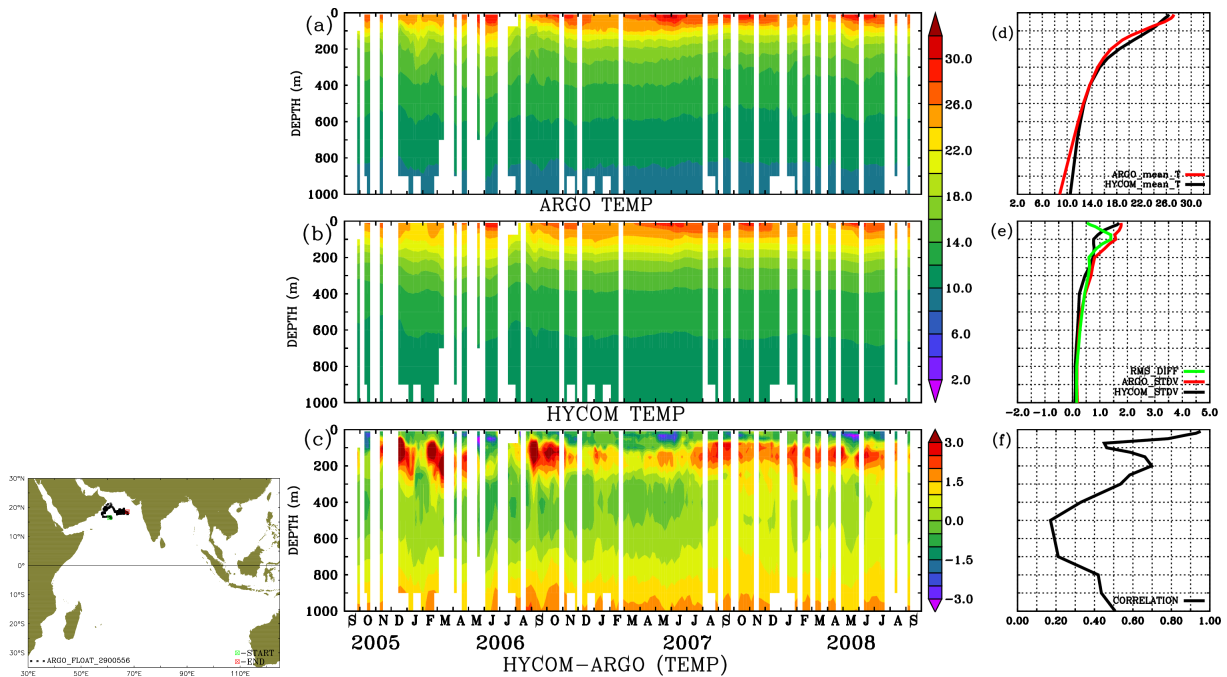


Figure 23: Time depth section of Argo float 2900556 compared against HYCOM temperature sampled at same locations and time

sections of temperature from Argo and temperature profiles sampled from HYCOM at the locations traversed by the float is presented in Figure - 23.

The float provides a relatively long time series of temperature starting from September 2005 up to September 2008, though there are several data gaps with missing profiles. The float made a relatively small geographical tour off the East African coast, moving closer to the coast traversing little bit along the coast and reached up to the central northern Arabian Sea. The temperature contours from the float is reproduced by the model with a good extend of similarity in case of events like the deepening of contours during September 2006 (Figure - 23, b, c). The mean profiles from both Argo and model are in reasonably good agreement. Both Argo and model standard deviation goes below 1°C for deeper layers below 400 meter depth. Maximum standard deviation are seen for depth above 200 meters in this region for both Argo and model temperatures. However model standard deviation is some what lower than the Argo standard deviation for the upper 200 meter which may be due to the sampling close to the coast. Compared to both standard deviations, RMS difference between HYCOM and Argo is much smaller for upper layers up to 100 meter depth where it reaches a maximum just close to the standard deviation of Argo temperature (Figure - 23). The correlation shows the maximum values above 100 meters but shows a sharp decline to 0.5 at 100 meters and then

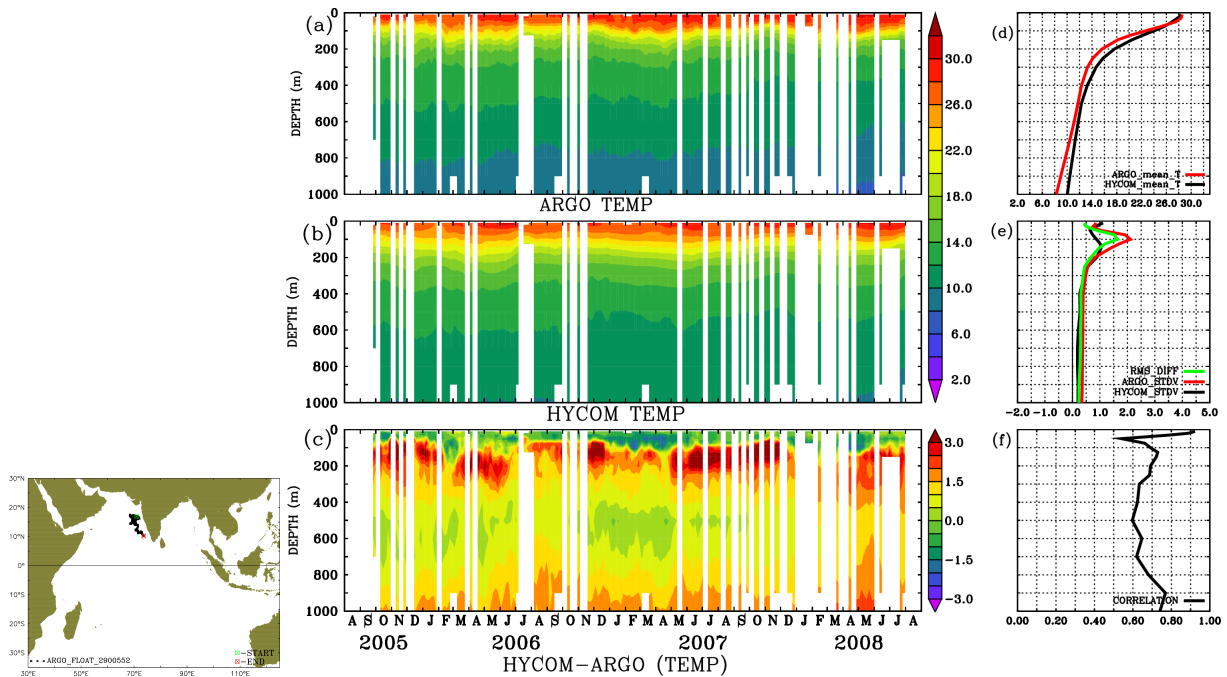


Figure 24: Time depth section of Argo float 2900552 compared against HYCOM temperature sampled at same location

reduces below 400 meter where the temperature variability goes below 0.5°C . The difference plot (Figure - 23, c) shows that the model is warmer for depths between 100 to 200 meters compared to Argo and there are few pockets where it goes above 3°C (e.g. December & February 2005 and also August & September 2006). From 200 meters to 800 meters model and Argo show very little differences in temperatures and there after near to 1000 meters the model become warmer ($\approx 1.5^{\circ}\text{C}$) again compared to Argo temperature.

For eastern Arabian sea close to Indian coast, Argo float 2900552 was chosen, which had a long time series of about 4 years starting from October 2005 to July (Figure - 24). The float was deployed at about 19°N and 70°E from where it moved towards south almost parallel to the Indian Coast. There were several gaps and the number of them increased after 2007. However the mean profile and the sections obtained from HYCOM gives a reasonable comparison with Argo temperature profiles, as evident from the temperature contours in Figure - 24(a, b, d). Many seasonal and sub-seasonal events exhibited by the sub surface temperature contours of Argo are also reproduced by the HYCOM temperature contours (Figure - 24 a, b). Compared to the western Arabian sea, the thermocline is less steep at this location. The standard deviation of temperature from the thermocline region is about 1.5°C more compared to the same of model. However the RMS difference is less than the standard deviation of the observation

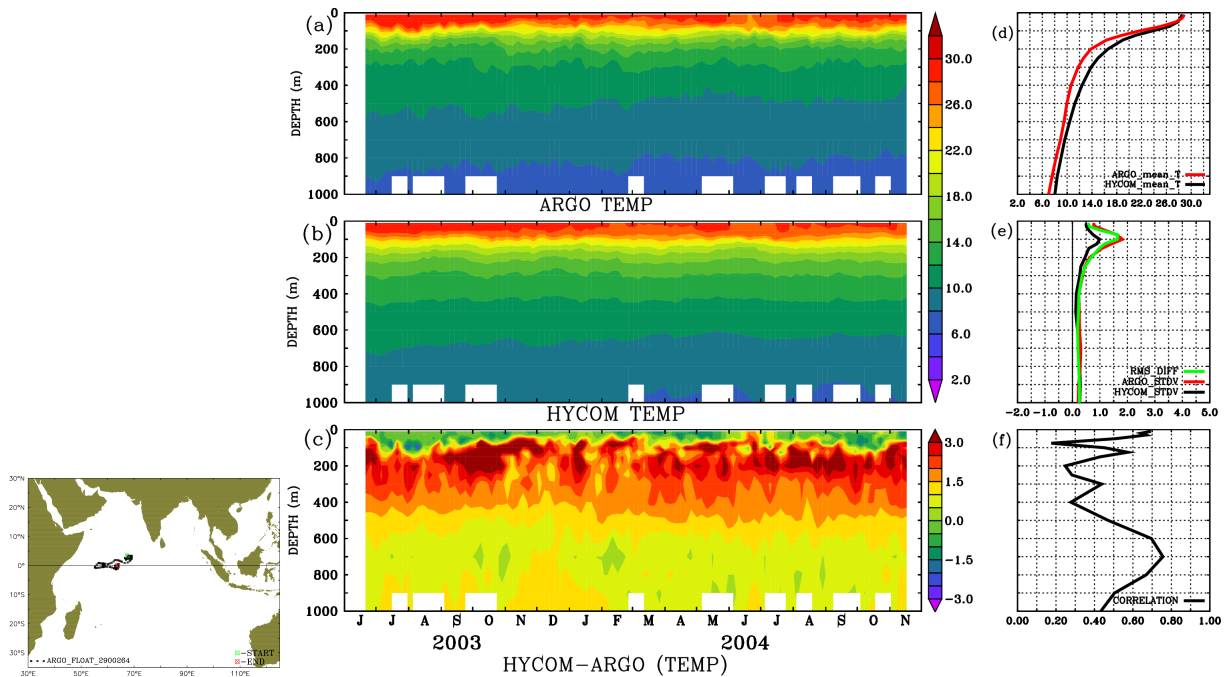


Figure 25: Time depth section of Argo float 2900264 compared against HYCOM temperature sampled at same location

through out the water column which shows a minimum close to surface. Below 200 meters, there is a sharp decline in standard deviation which goes below 0.5°C at this location. The correlation remains above 0.6 except for a sharp decline to 0.5 at about 50 meters, which 0.9 at surface and is about 0.75 for the depth below 800 meters up to 1000 meters. The Argo-model difference reach maximum close to depths between 100-200 meters and in the range of 1.5 to 2°C except for pockets where it goes above 3°C . There after model show minimum difference close to zero for depths from 400 to 800 meters. Except for near surface layers, the model is observed to be warmer compared to the Argo measured temperature throughout the water column.

Argo float:2900264 deployed slightly north of equator and sampled the Ocean from 50°E to 70°E has one and a half year time series of temperature measurements within this longitude belt. To assess the model performance in this region, equivalent HYCOM temperature profiles are compared with Argo and statistics were computed (Figure - 25).

The mean profile from both Argo float 2900264, and HYCOM present very good agreement up to a depth below 100 meters from surface (Figure - 25, d). Below 100 meters, there is region of difference between both profiles up to a depth of 600 m. In these layers too the maximum difference between the mean profile goes up to 0.8° (Figure- 25, d). At this location too the Argo temperature shows maximum standard deviation at 100 me-

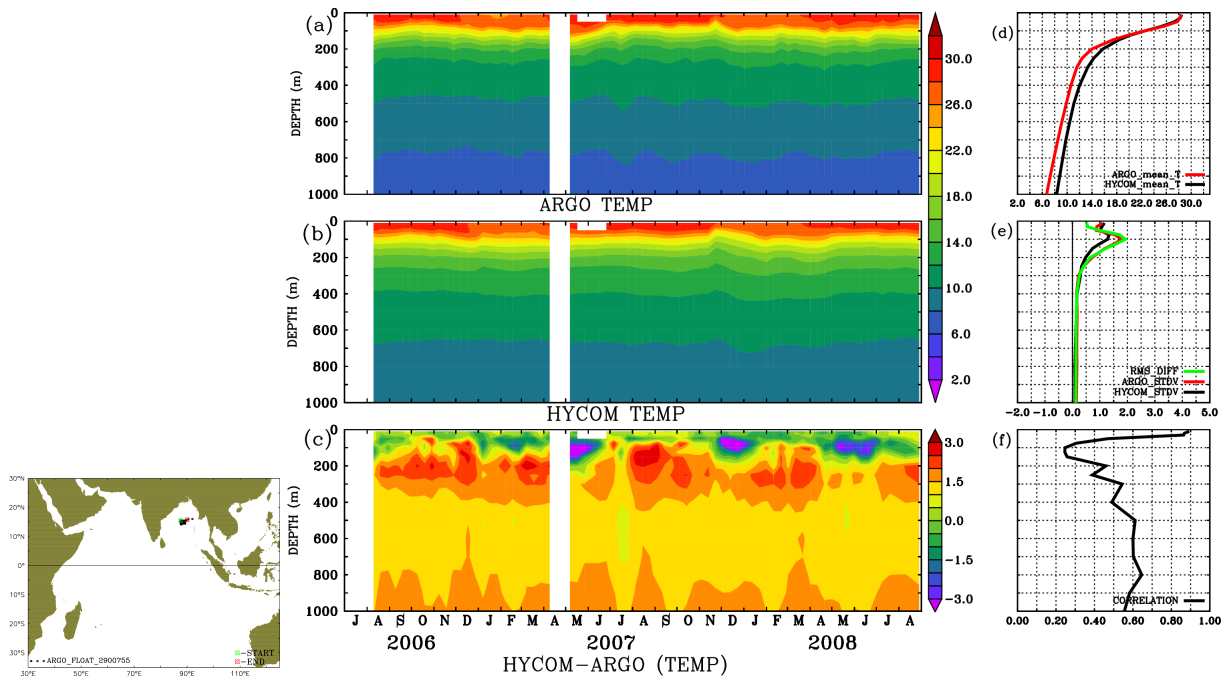


Figure 26: Time depth section of Argo float 2900755 compared against HYCOM temperature sampled at same location

ters reaching up to 1.9°C , where HYCOM shows a standard deviation of 1°C . There is a sharp decline in standard deviation below this depth and both Argo and HYCOM standard deviations fall below 0.5°C as the profiles goes down to 1000 meters. The correlation curve depicts very dramatic variability for the upper 400 meters, which shows a steady improvement and there after becoming equivalent to that of surface at 600 to 800 meter depth. These shifts in correlation could be due to the presence of Argo sampling at highly dynamic equatorial belt where under currents play a role in maintaining the thermohaline structure. Below the depth of about 50 meter the model is warmer compared to Argo temperature and there are pockets close to 150 meter where the difference go above 3°C . Apart from surface layers, the layers between 600 to 800 meters shows minimum difference between the two data sets.

For the Bay of Bengal region, Argo float No:2900755 which sampled ocean around 15°N with out much spatial drift, is chosen for cross validating model derived temperature field which is validated against RAMA buoy located at 15°N (Figure - 26). However the model data was sampled from the same locations where float sampled the Ocean around 15°N . Unlike other locations, float data is available here as a long time series with a single gap in April 2007, for about 3 years until August 2008. This region is characterized with a thermocline at about 120 meters (depth of 20°C isotherm), which is in good agreement with model. The tempera-

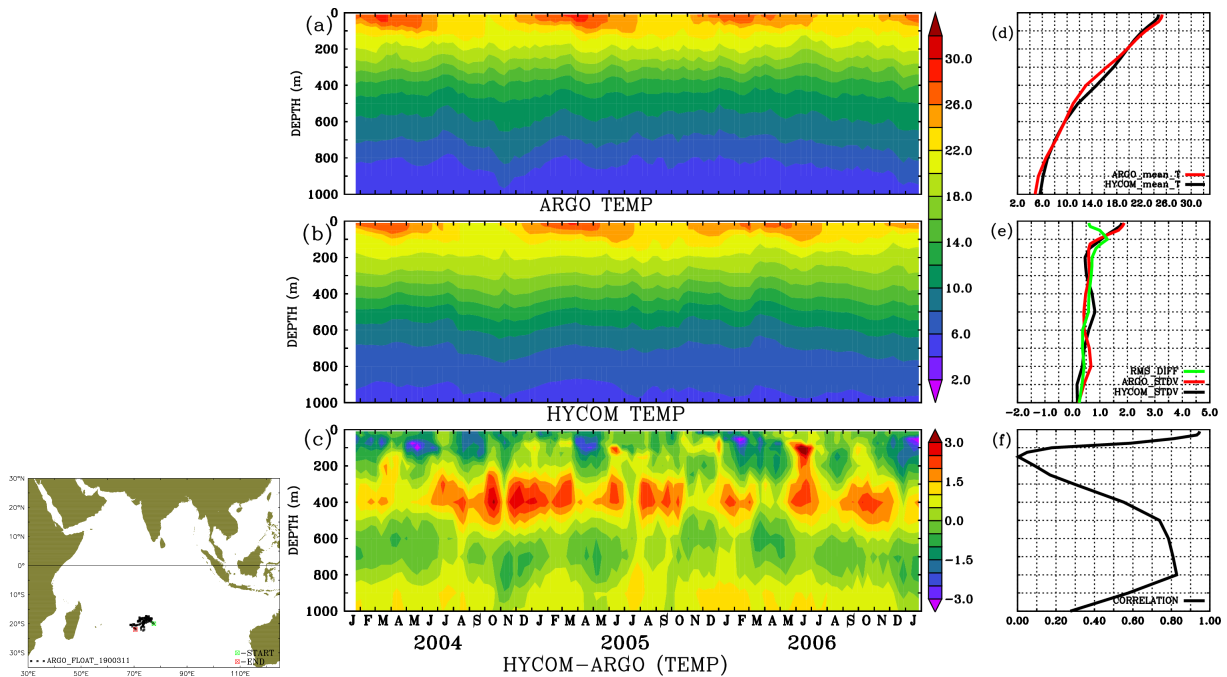


Figure 27: Time depth section of Argo float 1900311 compared against HYCOM temperature sampled at same location

ture contours of time depth section from both model and Argo are in good agreement. The difference is standard deviation between model and Argo at thermocline region is less than 0.5°C . However in case of RAMA, a single point measurement, the thermocline is some what deeper (≈ 150 m) compared to the mean of Argo profile samples. There is a sharp decline in temperature variability indicated by standard deviations falling below 0.5°C . The difference plot (Figure - 26(c)) shows that there are few small pockets at around 100 meters where the difference goes above 3°C . In general the model is warmer compared to Argo and the difference is seen maximum at about 200 m. Between 300 to 800 meter the Argo-model difference is minimum, which shows slight increase close to 1000 m. The correlation plot from Argo is significantly different and better compared to the RAMA mooring at the 15°N , which may be attributed to the comparison of point observation to the $1/4^{\text{th}}$ degree model which represent a rather broad scale variability which is better captured by the spatially moving Argo float. This can be further confirmed by the better comparison of the profiles from $1/12^{\circ}$ model with same vertical structure as that of $1/4^{\circ}$ with RAMA (not shown).

For southern Indian Ocean, Argo float No: 1900311 which had a time series of 3 years is chosen for comparison with the HYCOM (Figure - 26). Though the disturbances can be expected at this location due to the climatological relaxation at eastern boundary where Indonesian through

flow is blocked, the comparison with float data is reasonably good. Four distinct warming episodes associated with southern summer is clearly seen in both Argo and HYCOM for all the 3 years and beginning of the forth year. The mean profiles from both Argo and HYCOM shows a good match for the entire water column. The RMS difference is about 0.5°C for the layers close to surface where the standard deviation goes above 2°C . For the subsurface layers the standard deviations and RMSD remains less than 1°C through out the water column up to 1000 meters depth. The difference plot (Figure - 26 (c)) shows that the the model is slightly cooler compared to the Argo for the top 200 meters in general. It becomes warmer for layers between 300 m to 450 m and switches to relatively cool difference for layers from 450 to 800 meters and their after becoming warmer by about 1°C again. This pattern of warm cool switching of the Argo-model difference is particular to this southern ocean location. The correlation between the Argo and model is observed to be maximum at surface. It deteriorates to zero for a point location at 150 m and regain to 0.5 around 400 meters and reaches 0.82 at 800 meters. Thus there is a large scale depth variability exhibited at this location with respect to model performance in comparison with the Argo profiles.

6 Conclusions

Comparison of sea-level anomalies simulated by HYCOM and that of altimeter demonstrated the the model is able to reproduce the observed variability of sea-level in daily, monthly and inter annual time-scales. There are relatively large errors seen in model with respect to altimeter in areas of highly dynamic eddies like that of east African coast and Bay of Bengal. These locations can only be simulated better by use of suitable assimilation technique together with increase in resolution of model. RMS difference between HYCOM and altimeter is found to vary from 3 cm to 8 cm for regions other than the highly dynamic places.

Basin wide circulation in Indian Ocean is well represented in model simulated currents in Indian Ocean, in agreement with the OSCAR analysis which is produced from observations. Most of the seasonal characteristics of monsoonal circulation in Indian Ocean are present in HYCOM simulations, which is seen in the OSCAR analysis and close to the descriptions in the literature. The comparison of daily mean currents from HYCOM with the daily means of RAMA buoy currents show that the model has maximum skill in reproducing zonal currents close to the equator (0.68 at 80.5°E), and the performance is relatively lower as the sampling move away from

equator. In case of meridional currents, the maximum skill is observed at 4°S , 67°E , where HYCOM shows a skill of 0.5 against RAMA buoy measured currents.

The comparison of HYCOM SST with the observed TMI SST (for spatial comparison) on a monthly scale for the period 2003 to 2010 and RAMA buoys on a daily scale shows that the model is able to simulate the basin scale features of SST evolution spatially along with the temporal evolution on a daily time scale. The SST from both RAMA and HYCOM shows a very systematic pattern of variability across the equator in north south. The HYCOM SST shows maximum skill and correlation with respect to RAMA at the northern most site at 15°N , which gradually decrease to equator where high frequency variability plays a major role. It improves further as the samples are compared towards south.

The comparison of vertical profiles from RAMA with equivalents sampled from HYCOM demonstrated that the model reproduces the vertical thermal structure with good amount of accuracy. There is very good correspondence between HYCOM and RAMA mean profiles for the upper 200 meter at all three locations of RAMA locations which were compared with HYCOM. There is decline statistics for depths of 100 to 200 meter in comparison with depths above in all three cases. At all the three locations, the variability in the subsurface below 200 meter goes below 0.5° in both model and RAMA temperatures. The spatial correlation analysis at 80.5°C on equator show that the spatial correlation of temperature at this location is very localized and can result in poor performance due to the relative distance to the model grid point and location of observation.

Five representative argo floats are compared with HYCOM temperatures sampled at same locations and time in this report. The model compares well with the time mean Argo profiles in all the five cases and is in general warm for the sub-surface with respect to Argo profile temperature. The HYCOM simulation is relatively poor close to 200 meter depth with varying degree of difference with respect to time. The pattern of variability of model with respect to Argo float at around 20°S is significantly different from those of other northern location in exhibiting alternative warm and cool bias with respect to observed temperatures at this location.

In this report we are not presenting the comparison of Salinity with respect to observations as we have relaxed salinity to climatology.

From the critical analysis of model performance in comparison with observations and inferences from statistics, we suggest the following for the lacunae found in model simulations with observed variables.

- Increase the resolution of model taking care of the computational expenses, requirements and availability of suitable forcing.
- Replace the relaxed boundaries at the eastern, southern and western side of the model with boundary conditions from a global model.
- Implement assimilation of sea level and SST data along with vertical profiles of temperature and salinity.

7 Acknowledgements

Director, INCOIS is thanked for the suggested corrections and infrastructural support. Dr. Shailesh Nayak secretary Ministry of Earth Sciences(MOES) is acknowledged for his encouragement during his tenure as INCOIS director as well as in present position. Dr. Alan Wallcraft of Naval Research Laboratory (NRL), USA us acknowledged, for numerous email exchanges during the initial setup of the model in newly acquired HPC at INCOIS. Colleagues at INCOIS are acknowledged for their support.

References

- Antonov, J., S. Levitus, T. P. Boyer, M. Conkright, T. O' Brien, C. Stephens, and B. Trotsenko, Temperature of the indian ocean. vol. 3, world ocean atlas 1998, in *NOAA Atlas NESDIS 29*, p. 166 pp., U.S. Gov. Printing Office, Washinton, D. C., 1998.
- Barron, C. N., and L. F. Smedstad, Global river inflow within the navy coastal ocean model, in *Proceedings, MTS/IEEE Oceans 2002 Conference*, pp. 1472–1479, doi:<http://www7320.nrlssc.navy.mil/pubs/2002/barron-paper.pdf>, 2002.
- Bleck, R., An oceanic general circulation model framed in hybrid isopycnic-cartesian coordinates, *Ocean Modelling*, *4*(1), 55–88, 2002.
- Bonjean, F., and G. S. E. Lagerloef, Diagnostic model and analysis of the surface currents in the tropical pacific ocean, *J. Phys. Oceanogr.*, *32*(10), 2938–2954, 2002.
- Bruce, J., Notes on the somali current system during the southwest monsoon, *J. Geophys. Res.*, *75*(21), 4170–4173, 1970.
- Bruce, J. G., Eddies off the somali coast during the southwest monsoon, *J. Geophys. Res.*, *84*, 7742–7748, 1979.
- Cutler, A., and J. Swallow, Surface currents of the indian ocean (to 25°s, 100°e): compiled from historical data archived by the meteorological office bracknell, uk., *Technical Report 187*, Institute of Ocean Sciences, Wormley, UK, Institute of Oceanographic Sciences, 1984.
- Donguy, J., and G. Meyers, Observations of geostrophic transport variability in the western tropical indian ocean, *Deep-Sea Res. Part I*, *42*(6), 1007–1028, 1995.
- Halliwel, G. R., Decadal and multidecadal north atlantic sst anomalies driven by standing and propagating basin-scale atmospheric anomalies, *J. Climate*, *10*(10), 2405–2411, 1997.

- Haugen, V. E., O. M. Johannessen, and G. Evensen, Mesoscale modeling study of the oceanographic conditions of the southwest coast of india., *Earth and Planetary Sci.*, *111*(3), 321–337, 2002a.
- Haugen, V. E., O. M. Johannessen, and G. Evensen, Indian ocean: Validation of the miami isopycnic coordinate ocean model and enso events during 1958-1998, *J. Geophys. Res.*, *107*, C5–3043, doi:10.1029/2000JC000330, 2002b.
- Large, W. G., J. C. McWilliams, and S. C. Doney, Oceanic vertical mixing: A review and a model with a nonlocal boundary layer parameterization, *Reviews of Geophysics*, *32*(4), 363–403, cited By (since 1996): 570, 1994.
- Schott, F., and J. P. McCreary, The monsoon circulation of indian ocean, *Progress in Oceanogr.*, *51*, 1–123, 2001.
- Shankar, D., P. N. Vinayachandran, A. Unnikrishnan, and S. R. Shetye, The monsoon currents in the north indian ocean, *Progress in Oceanogr.*, *52*(1), 63–120, 2002.
- Shenoi, S., P. Saji, and A. Almeida, Near-surface circulation and kinetic energy in the tropical indian ocean derived from lagrangian drifters, *J. Mar. Res.*, *57*(6), 885–907, 1999.

Appendix - I

Quality Codes:

RAMA current data quality varies as the instrument operate in a dynamic environment. So it is important to see the quality flags before making conclusion regarding the compared data. Daily mean data we used in this report are computed from all available high resolution data over a 24-hour interval beginning at 0000 GMT. Time stamps associated with these data are the middle of the interval (1200 GMT).

0 = datum missing

1= highest quality; Pre/post-deployment calibrations agree to within sensor specifications. In most cases only pre-deployment calibrations have been applied

2= default quality; Pre-deployment calibrations applied. Default value for sensors presently deployed and for sensors which were either not recovered or not calibratable when recovered.

3= adjusted data; Pre/post calibrations differ, or original data do not agree with other data sources (e.g., other in situ data or climatology), or original data are noisy. Data have been adjusted in an attempt to reduce the error.

4= lower quality; Pre/post calibrations differ, or data do not agree with other data sources (e.g., other in situ data or climatology), or data are noisy. Data could not be confidently adjusted to correct for error.

5= sensor or tube failed

The quality flags of the selected RAMA buoys for zonal and meridional current time series analysis and statistics generation are presented in Figure - 28 below.

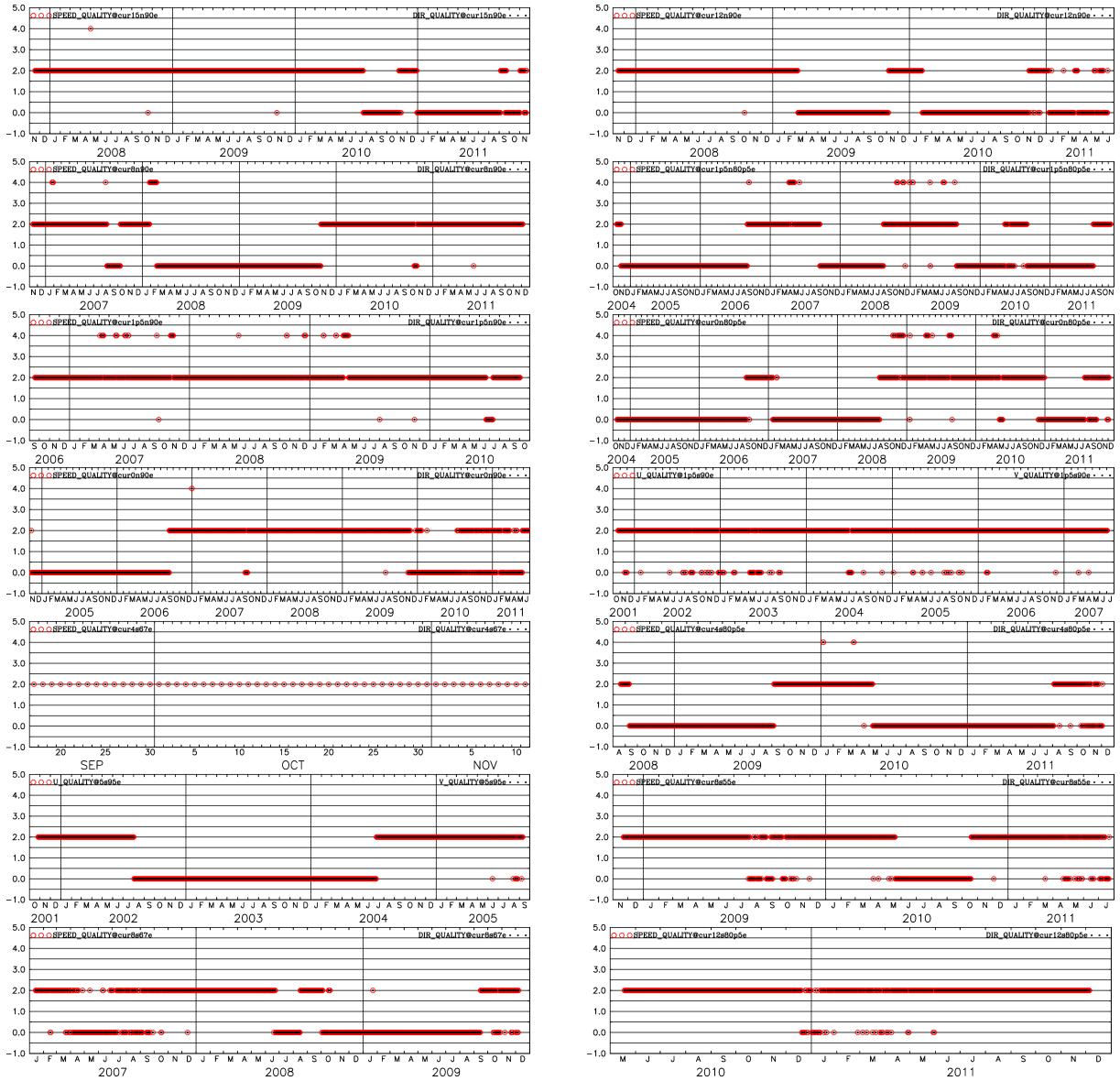


Figure 28: Quality flags of RAMA Buoy currents used for comparison with HYCOM current time series(R-01 to R-14 ,Figure-12)